PROPAGATION OF IONIZING SHORT LASER PULSES IN A NONLINEAR OPTICAL MEDIUM

A THESIS SUBMITTED TO
THE GRADUATE SCHOOL OF NATURAL AND APPLIED SCIENCES
OF
MIDDLE EAST TECHNICAL UNIVERSITY

BY

ATALAY DEVECI

IN PARTIAL FULFILLMENT OF THE REQUIREMENTS
FOR
THE DEGREE OF MASTER OF SCIENCE
IN
PHYSICS

FEBRUARY 2021

Approval of the thesis:

PROPAGATION OF IONIZING SHORT LASER PULSES IN A NONLINEAR OPTICAL MEDIUM

submitted by **ATALAY DEVECI** in partial fulfillment of the requirements for the degree of **Master of Science in Physics Department, Middle East Technical University** by,

Prof. Dr. Halil Kalıpçılar
Dean, Graduate School of **Natural and Applied Sciences** _____

Prof. Dr. Altuğ Özpineci
Head of Department, **Physics** _____

Assoc. Prof. Dr. Burak Yedierler
Supervisor, **Physics, METU** _____

Examining Committee Members:

Assoc. Prof. Dr. Kemal Efe Eseller
Electrical and Electronical Engineering, Atılım University _____

Assoc. Prof. Dr. Burak Yedierler
Physics, METU _____

Prof. Dr. İsmail Rafatov
Physics, METU _____

Date: 15.02.2021

I hereby declare that all information in this document has been obtained and presented in accordance with academic rules and ethical conduct. I also declare that, as required by these rules and conduct, I have fully cited and referenced all material and results that are not original to this work.

Name, Surname: Atalay Deveci

Signature :

ABSTRACT

PROPAGATION OF IONIZING SHORT LASER PULSES IN A NONLINEAR OPTICAL MEDIUM

Deveci, Atalay
M.S., Department of Physics
Supervisor: Assoc. Prof. Dr. Burak Yedierler

February 2021, 62 pages

Using a pseudo-spectral method that is split step Fourier method, obtaining a solution for propagation of ionizing short Gaussian pulse would be computationally inexpensive and practical. For a solution obtained by using split step Fourier method, the most important parameter to choose is step size. However, using either large or small step size may yield different numerical errors in the final result. For a large step size, general evolution of the Gaussian pulse could be predicted well but small changes might be neglected. for a small step size, small changes could be indicated well but there would be a prone to error in general pulse evolution. Furthermore, using a generic method of undetermined coefficients that could be utilized for every differential equation would yield a high accuracy solution in order to check the validity of split-step Fourier method.

The aim of this study is to examine the evolution of the ionizing short Gaussian pulse lasers in a non-linear medium in both low intensity propagation regime and high intensity propagation regime via various methods to solve the propagation equation *i.e* split-step Fourier method and method of undetermined coefficients. Similarity of two solutions arising from split-step Fourier method and method of undetermined coef-

ficients would evolve in a similar trend. Comparison of solutions for both gathered from split-step Fourier method and method of undetermined coefficients with the previous solutions from the literature in the low intensity propagation regime are behave similar except some pulse parameters. Difference between in the parameters of the Gaussian pulse in low intensity propagation regime and high intensity propagation regime has been shown.

Results would be given in terms of the pulse parameters *i.e* spot size, pulse length, intensity, power, electron number density, field amplitude and energy. These results would be used for whether split-step Fourier method and method of undetermined coefficients match the expectancy. Evolution that could be derived by these two different methods fulfill the expectancy, that is expected power loss, expected energy loss and shorter focus length.

Keywords: Gaussian pulse evolution, Nonlinear optics, Physics of plasmas, Ionization by Gaussian pulses in air

ÖZ

İYONLAŞTIRICI KISA LAZER ATIMLARININ DOĞRUSAL OLMAYAN ORTAMDA YAYILIMI

Deveci, Atalay
Yüksek Lisans, Fizik Bölümü
Tez Yöneticisi: Doç. Dr. Burak Yedierler

Şubat 2021 , 62 sayfa

İyonize edici kısa Gauss atımının yayılışı bir çözüm elde etmek için, split-step Fourier yöntemi olan sözde spektral bir yöntem kullanmak, hesaplama açısından kolay ve pratik olacaktır. Split-step Fourier yöntemi ile bulunan bir sonuçta seçilmesi gereken en önemli parametre ise adım boyutudur. Ancak, büyük veya küçük adım boyutu kullanmak, nihai sonuçta farklı sayısal hatalara neden olabilir. Büyük bir adım boyutu için, Gauss sinyalinin genel evrimi iyi tahmin edilebilir, ancak küçük değişiklikler ihmal edilebilir. Küçük bir adım boyutu için, küçük değişiklikler iyi bir şekilde gösterilebilir, ancak genel atım gelişiminde hataya yatkınlık olacaktır. Ayrıca, her diferansiyel denklem için kullanılabilecek jenerik bir yöntem olan belirsiz katsayıların kullanılması, split-step Fourier yönteminin geçerliliğini kontrol etmek için yüksek doğrulukta bir çözüm sağlayacaktır.

Bu çalışmanın amacı, iyonlaştırıcı kısa Gauss atımlı lazerlerin doğrusal olmayan bir ortamda, hem düşük yoğunluklu yayılma rejiminde hem de yüksek yoğunluklu yayılma rejiminde evrimini çeşitli yöntemlerle, yani split-step Fourier yöntemi ve belirsiz katsayılar yöntemini kullanarak yayılma denklemini çözmektir. Split-step Fourier

yönteminden ve belirsiz katsayılar yönteminden kaynaklanan iki çözüm, benzer bir eğilim içinde gelişecektir. Hem split-step Fourier yönteminden hem de belirlenmemiş katsayı yönteminden elde edilen çözümlerin, düşük yoğunluklu yayılma rejiminde literatürdeki önceki çözümlerle karşılaştırılması, bazı atım parametreleri dışında benzer davranmaktadır. Düşük yoğunluklu yayılma rejiminde ve yüksek yoğunluklu yayılma rejiminde Gauss atım parametreleri arasındaki fark gösterilmiştir.

Sonuçlar, nokta boyutu, atım uzunluğu, yoğunluk, güç, elektron sayı yoğunluğu, alan genliği ve enerji gibi atım parametreleri açısından verilecektir. Bu sonuçlar, split-step Fourier yönteminin ve belirlenmemiş katsayıların yönteminin beklentiye uygun olup olmadığı için kullanılacaktır. Bu iki farklı yöntemle elde edilebilecek evrim, beklenen güç kaybı, beklenen enerji kaybı ve daha kısa odak uzunluğu beklentisini karşılamaktadır.

Anahtar Kelimeler: Gauss atımlarının evrimi, Doğrusal olmayan optik, Plazma fiziği, Havada gerçekleşen ve Gauss atımlarından kaynaklanan iyonizasyon

To my family, to my future wife and to my dearest friend.

ACKNOWLEDGMENTS

I would like to thank to my supervisor, Burak Yedierler, that not only to lead me to complete this study, but also he was a mentor to me and an idol to how to think skeptically in life. Although I have shifted my career goals from physics to a different branch, machine learning, he supported and encourage me to utilize the aspect that I learned in physics to machine learning. He has changed the way I see how an academic should look and behave like. I feel grateful that I had the privilege to work and study with him.

My dearest mother, Sevgi and father, Ali have supported me to the extremes. I believe no one has such a support from their family. Without their support, I believe I could not be able to finish this study with success. They are also the cause that I was so interested in natural sciences and statistics which is their profession. I owe them for my aspect of to think skeptically to every problem that I encounter.

The love of my life, Ecem, have supported me in all manners. She always convinced me that I am capable to deal with all the struggles that I have. Without her support, both this study and my other successes were not possible.

Kıvanç, who is the only true friend that I have encouraged me to enhance my skills in physics and extremely supported for both this study and in daily life in any cases. He is a great friend, a great intellectual and a great idol...

Also, I would like to thank to all the members of Biokido where I am working right now as a machine learning engineer. Especially Özgür, who is my boss, supported me to finish this study without reminding me the responsibilities in workplace and Sarper, who is my project lead, supported me that I am capable.

TABLE OF CONTENTS

LIST OF TABLES

TABLES

LIST OF FIGURES

FIGURES

LIST OF ABBREVIATIONS

LIPR	Low intensity propagation regime
HIPR	High intensity propagation regime
MUC	Method of undetermined coefficients

CHAPTER 1

INTRODUCTION

Electromagnetic wave propagation in many different media has been already explained in detail since the 19.th century. J. C. Maxwell has introduced Maxwell's equations for electrodynamics that explain the electromagnetic wave propagation in a medium. After most of the dynamics for electromagnetic wave have been introduced, such as diffraction, reflection, and refraction, some has noticed that these dynamics are not sufficient to explain the propagation of the electromagnetic waves if the medium has certain conditions. These conditions are related to the internal and external properties of the medium. For example, if there are ionized particles in the medium in which the wave propagates, explaining the propagation of the medium is not sufficient. Another example could be whether the particles have a speed near the relativistic effects take place. All those physical phenomenons change the way of propagation of the electromagnetic wave. Therefore, introducing novel terms to Maxwell's equations became mandatory. Overall, all of these effects could be said to be the polarization effects of the medium. These polarization effects could be named as the ionized particle in the medium, relativistic effects, Kerr effect, ion creation by the electromagnetic wave, energy depletion due to ionization, and Raman effect. These effects are named nonlinear effects of the optical medium.

By the introduction of new phenomenons related to the polarization effects of the medium, constructing a new propagation equation became possible. However, polarization effects also change with the shape of the wave. Since there are multiple types of waves that both studied and used in industry for commercial uses, such as sine waves, square waves, triangular waves, Gaussian waves *etc.*, investigating those different shapes of electromagnetic waves yield a different evolution in the medium.

Furthermore, it could be stated that for a chosen shape of the electromagnetic wave, some of the internal parameters, such as intensity, change the importance of the polarization terms in the propagation equation. For example, if the intensity is sufficiently high for a Gaussian wave, all of the polarization terms have to be taken into account in order to determine the evolution of the electromagnetic wave. However, if the intensity of the wave is not sufficient, Raman effects, ion creation effects, ion density effects, relativistic effects, and energy depletion by ionization effects could be neglected. However, for such a case, the intensity may be sufficiently high to observe Kerr effect. Therefore, every different nonlinear effect for polarization may have different thresholds for the internal properties of the electromagnetic wave.

One of the most important nonlinear effects could be said to be Kerr effect. If investigated properly, one could state that Kerr effect and diffraction of the propagating electromagnetic wave have a conflict between themselves. Although it is clearly known that propagating wave diffracts in the medium, that is wave amplitude shrinks and the wave defocuses in time throughout the evolution, Kerr effect does the opposite. However, for a Gaussian wave that has sufficiently high intensity, Kerr effect overcomes the diffraction effect and yields a focusing wave instead of a defocusing wave. The region where this phenomenon occurs is called *Low Intensity Propagation Regime(LIPR)*. In low intensity propagation regime, propagating electromagnetic wave self-focuses because of the overcoming Kerr effect. Therefore, this self-focusing effect increases the intensity of the wave further while propagating. In low intensity propagation regime, the intensity is not sufficient to ionize the region, ion creation, and energy depletion effects, then those could be neglected. However, if a critical intensity is achieved, ionization effects become significant if one compares it with the Kerr effect. At that threshold, the medium could be ionized by the self-focusing electromagnetic wave. While ionization occurs, Kerr effect is dominated by ion creation, electron number density, and energy depletion effects. The region where this phenomenon occurs is called *High Intensity Propagation Regime*(HIPR). Therefore, one could state that different regimes could be well-distinguished by whether Kerr effect dominates diffraction effect or ionization effects dominates Kerr effect.

Low intensity propagation regime has been studied and explained in detail by the contributions from Sprangle *et al.* Chin *et al.*, Yedierler and Aközbek *et al.*. The

propagation equation for specifically a short and intense Gaussian pulse only consists of one additional polarization effect, which is Kerr effect. Also, these studies have been done by utilizing different methods to solve the propagation equation. These methods consist source-dependant expansion[36], variational analysis[2, 41, 42, 43] and method of undetermined coefficients[35]. Although it is possible to utilize numerical approaches for that problem, such as the central finite difference method, it is not necessarily important to solve a propagation equation that could be solved semi-analytically. However, solutions for high intensity propagation regime require tedious work with semi-analytical approaches. Therefore, a powerful pseudo-spectral method, which is split-step Fourier method has been utilized to solve the propagation equation in high intensity propagation regime by Feng *et al.*. Hence, a semi-analytical approach for the evolution of a short pulse laser has not been proposed before.

Although it requires certain assumptions and tedious work to solve the propagation equation in high intensity propagation regime, it is possible to utilize a solution using the method of undetermined coefficients. The solution gathered from the method of undetermined coefficients is not only a novel approach for this problem but also a confirmatory result for split-step Fourier method. Therefore, the solution for the propagation equation for a short laser pulse in a nonlinear optical medium is highly important in order to explain the remote ionization caused by the high intensity of the pulse in a specific region. This remote ionization could be used in many different areas which will be mentioned below ranging from industry to medical usage. These applications diverge in terms of the number of ionized particles in the ionization region of short pulse lasers. In order to precisely define the number of ionized particles in the ionization region of short pulse lasers, one must solve the propagation equation of the short pulse laser in the nonlinear optical medium which directly depends on the number density of ionized particles in the medium.

In this study, the only method of undetermined coefficients and split-step Fourier method will be investigated. There are several advantages and disadvantages to use the method of undetermined coefficients and split-step Fourier method. For split-step Fourier method, obtaining the wave parameters that have a spatial dependency, such as spot size, pulse length, power, curvature, and chirp, are not required to be found explicitly in the functional form. Only utilizing the initial values are highly

sufficient since these methods iteratively solve the system of propagation equation numerically. Therefore, it yields only the field amplitude and number density depending on field amplitude. However, if split-step Fourier method has decided to be used, one must decide the parameters of the split-step Fourier method, most importantly the step size. Since step size determines the precision of the solution, choosing a high value for step size yields poor precision in small distances. Conversely, choosing a small step size yields a high precision, but it makes the system completely false due to an error is known as an exploding gradient. Furthermore, even if there will be no exploding gradients while numerically solving the system, small step size is computationally expensive. Therefore, tuning the parameters for split-step Fourier method is extremely vital. For the method of undetermined coefficients, one could say that it requires more effort than utilizing split-step Fourier method since it requires the spot size, pulse length, power, curvature, and chirp functions explicitly. Therefore, utilizing the method of undetermined coefficient requires a system of equations with the same number of unknowns. After finding those equations and unknowns, one could state that some exponential terms in those equations are highly problematic and needed to be eliminated before using a mathematical solver such as $Mathematica^{TM}$. Apart from the error due to Taylor expansion of the exponential terms in the differential equations, the method of undetermined coefficient one advantage over split-step Fourier method, which is being able to examine the whole propagation evolution in terms of spot size, pulse length, power, energy, and intensity. Examining those parameters brings a clearer picture of whether the propagating wave in the low intensity propagation regime or high intensity propagation regime.

1.1 Short Pulse Lasers

Short laser pulses are electromagnetic waves that having a high frequency and high energy carrying potential. The time limits of short laser pulses are in the range of nanoseconds(*ns*) to femtoseconds(*fs*)in commercial forms. Application fields of these short laser pulses are in a wide range from time-resolved measurements, fiber optic communication, ionization by short pulses[28] *etc.*. Short pulse lasers are generated in a mode-locked laser oscillator in the front and its energy is amplified[15]. Some of

the application fields of short pulse lasers are listed below[20].

Some of the applications are using the propagation properties, some of which are using the ionization effects of propagation. Listed applications would be explained in detail below.

1.1.1 Manufacturing

In industry, lasers are widely used for several different tasks such as hardening the material by heating, welding, cladding, processing of microdevices, drilling and, cutting[20, 47]. Laser intensity is ranging $10^3 W/cm^2$ to $10^9 W/cm^2$ for different tasks[4, 37] For example, high-intensity femtosecond lasers could be used for cleaning the surface since these lasers do not heat the surface while interacting with the surface.[19, 20]. For example, if one's goal is to process the microchips, there are several advantages to use short pulse lasers in order to achieve that goal. One is the absence of thermal effects around the focal point. Since thermal effects may lead to a degeneration in the chip where is not the focal point of the laser, it is an advantage to use short pulse lasers while processing microchips. Furthermore, multiphoton absorption could be used to generate various structures on the surface, which is to use the ionization property of the short pulse lasers[47]. Another example is to glass process, which is to drill, to profile, or to cut. Since glass is highly sensitive in terms of its thermal properties to work with using a short pulse laser may lead to negligible thermal effects around the focal point as stated above[21].

1.1.2 Surgical Usage

In surgical usage, short pulse lasers could be used as some equipment for processing the tissues since collateral damage may be given with the standard types of equipments[20]. Proper usage of short pulse lasers as a scalpel with eye surgery could be shown as Laser-Assisted In-Situ Keratomileusis(LASIK)[20, 27]. By utilizing short pulse lasers, thermal effects are not a concern outside of the focal point. For the focal point, it cuts the region with the thermal effects, which is the desired outcome. Furthermore, short pulse lasers could also be used for scar therapies in order

to minimize the leftovers from surgery or any scar in terms of cosmetically. Since ionization effects could be used both for cutting and drilling, it could be used as a welding tool in human tissue as well[22]. Also, results from these studies are promising since it is possible to achieve better accuracy and precision with short pulse lasers than scalpels for surgery and some chemicals with scar therapy. Therefore, one could conclude that the thermal effects of the short pulse lasers are preferable since there is negligible collateral damage given to healthy or undesired to process regions of human tissue. With the minimal effect of thermal effects except for focal point, short pulse lasers could be also used as a promising tool instead of traditional radiology methods to cure cancer which will be mentioned below.

1.1.3 Ultrafast X-Ray Radiography

Since the arising point of a short pulse laser could be very small and approximated as a point, they could yield a coherent source of X-ray[20]. Spatial coherency of X-rays is one of the most important features for monitoring the tissue since this imaging technique makes use of phase shifts arising from different tissues like bones, muscles, etc. Therefore using a computer-based tomography and constructing the 3D image of the laser-tissue interaction would yield the contrast between healthy tissue and tumors in body[8, 13, 38, 40]. Furthermore, using ultrafast x-ray radiography allows examining the tissue in atomic scales where dynamical changes in tissue could be investigated further unlike being able to investigate only valance and free electron structure. One of the most powerful methods to use ultrafast x-ray radiography is to use the K-Alpha x-ray source which is created by the interaction between the ultrashort laser pulse and high-Z solid target[17]. Also, another method for ultrafast x-ray radiography is laser wakefield x-ray based radiography. This method relies on the laser wakefield acceleration of the electrons[17].

1.1.4 Electron Beams for Cancer Therapy

Selectivity while killing the cancer cells is an extremely important parameter. In classical radiotherapy, selectively killing cells is a problematic goal since collateral

damage given by highly energetic wave is enormous. However, recent studies in laser science stated that selectively killing cancer cells are plausible. One level of the selectivity could be achieved by focusing electrons into a designated point to minimize the collateral damage. Hence, focusing high energy electrons created by high intensity lasers using laser wakefield acceleration in plasmas could change the way of how radiotherapy will be done[20, 24]. This method could be expanded into two main mechanisms that explain the electron acceleration by laser wakefield. These are the Betatron and Inverse Compton emissions[17]. In order to achieve such electron acceleration by plasma wakefield, the intensity of the pulse have to reach a critical point where it lies between $10^{18} - 10^{20} W/cm$ in order not to neglect the effects of the laser wakefield source terms in the propagation equation. Therefore, either initial pulse intensity has to be sufficiently high, or the nonlinear Kerr effect has to focus the initial pulse more.

1.1.5 Ion Beams for Cancer Therapy

Using ion beams are one of the most convenient methods in cancer therapy since the stopping distance of ions is well-studied in human tissue. Therefore, it could be focused on a tumorous tissue to maximize the damage done to the tumor and minimize the collateral damage done to healthy cells around[20, 30, 44, 45]. One method is to use an ultrashort laser pulse to the thin foil target. When an ultrashort laser pulse interacts with a thin metal foil, electrons in the foil start to move and create a surface current and yielding a magnetic field. This magnetic field makes surrounding ions accelerates that is supplied by *e.g* hydrogen[16].

1.1.6 Pulse-based Ionization for Cancer Therapy

This method only uses the non-linear effects of the medium, *i.e* human tissue for this case to focus a non-heating short pulse laser on a specific spot. By doing so, a surgical operation may not be necessary to remove the tumorous region. Selectively ionizing the region where the tumor resides would only cause the death of the cancer cells with minimal collateral damage. While methods like ion beams require certain cancer

types like skin cancer since such an ion therapy cannot be done without explicitly opening the human tissue with surgery, pulse-based ionization only ionizes the region where the tumor is located[14].

Another technique to further increase the selectivity in killing cancer cells may be related to the insulin receptors around cancerous cells. It is proven that the density of insulin receptors are way higher than healthy cells[25, 29], detecting the density of insulin receptors via another laser pulse is plausible. Therefore it yields more selectivity while ionizing the region.

1.2 Aim of This Study

Motivation of this study is to show the evolution of short pulse lasers in a non-linear medium by taking ionization effects into account using two main methods that could be listed by

- Method of undetermined coefficients
- Split-step Fourier method

This study also contains full simulations of pulse evolution from low intensity propagation regime to high intensity propagation regime which studied separately in the literature. Also, long range propagation of short pulse lasers would be investigated.

CHAPTER 2

MATHEMATICAL MODEL

2.1 Gaussian Pulses

One of the most used models to represent short laser pulses is the Gaussian pulses. Gaussian pulses are waveforms that obeys the Gaussian distribution [39, 3, 12] that is in the form of $Aexp(-\frac{t^2}{T^2})$. Since Gaussian distribution is one of the simplest mathematical model and easy to modify it with external parameters such as curvature and chirp, it is widely chosen waveform to model a short laser pulse.

In this study, an initial chirped and having an initial curvature Gaussian pulse will be used as an input pulse. Curvature would be investigated only in focusing ($\alpha_0 > 0$) form[42, 43]. Mathematical expression of the input Gaussian short laser pulse could be shown as[35, 42, 43]

$$\epsilon(r,z,\tau) = \sqrt{\frac{16P(z)}{cn_0R^2(z)}}exp\left(i\phi(z) - \frac{(1+i\alpha(z))r^2}{R^2(z)} - \frac{(1+i\beta(z))\tau^2}{T^2(z)}\right) \quad (2.1)$$

where $\epsilon(r,z,t)$ is the field amplitude, $P(z)$ is the laser power, c is the speed of light, n_0 is the linear refractive index of the medium, $R(z)$ is the spot size, $\phi(z)$ is the phase function, $\alpha(z)$ is the curvature function, $\beta(z)$ is the chirp function, r is the radius of the pulse and τ is the proper time expressed as $\tau = t - z/v_g$ where t and v_g are time and group velocity respectively.

A complete explanation of the components for the electromagnetic wave would be investigated further in the *Chapter 2* since this only represents the field amplitude that is used as a fraction of the electric field.

2.2 Propagation Equation

As far as electrodynamics has concerned, every propagation equation is derived from Maxwell's equations. Therefore, including a source term, resulting propagation equation is in the form such that[35, 1, 2, 33]

$$\left(\nabla_{\perp}^{2} + \frac{\partial^{2}}{\partial z^{2}} - \frac{1}{c^{2}}\frac{\partial^{2}}{\partial t^{2}}\right)\boldsymbol{E} = \boldsymbol{S} \tag{2.2}$$

where $\nabla_{\perp}^{2}$ is the Laplacian over the perpendicular axis, $\boldsymbol{E}$ is the electric field and $\boldsymbol{S}$ is the source term. Source terms can be expanded in a way that $S = S_L + S_{NL}$ where S_L is the linear source term and S_{NL} is the non-linear source term. These linear and non-linear sources can be expanded further in order to have an explicit form of propagation equation. Physical phenomenons that govern the source terms could be identified related to their linearity[35, 34, 1, 41]. These terms would be discussed in the next section.

2.2.1 Linear Source Term Expansions

S_L can be expressed as[35, 1]

$$S_L(r,t) = \left(\frac{\omega_0}{c}\right)^{2} \sum_{l}^{\infty} i^{l}\alpha_l(r)\omega_0^{-l}\frac{\partial^{l}A(r,t)}{\partial t^{l}} \tag{2.3}$$

where $l = 0, 1, 2, 3...$, ω_0 is the initial angular velocity. As far as the conventional dispersion parameters are concerned [1], $\beta_l = \partial^{l}[(\omega/c)n_0(\omega)]/\partial\omega^{l}|_{\omega=\omega_0}$; α_l could be shown as

$$\alpha_l = -\frac{\omega_0^{l-2}}{l!}\frac{\partial^{l}}{\partial\omega_0^{l}}(c^{2}\beta^{2}(\omega_0) - \omega_0^{2}) \tag{2.4}$$

where $n_0(\omega)$ is the refractive index. It is possible to approximate α_l and β_l to the intended order. For this work, until β_2 would be approximated since higher order terms would be diminishing.

2.2.2 Non-linear Source Term Expansions

As it is stated before, non-linear terms would be named after their physical phenomenons. These are;

- Kerr effect
- Raman scattering
- Plasma source term
- Wakefield
- Relativistic effect
- Energy-depleting ionization

Therefore, total source term can be expressed as[34, 35]

$$S_{NL} = S_{Kerr} + S_{Raman} + S_{plasma} + S_{wake} + S_{rel} + S_{ion} \tag{2.5}$$

2.2.2.1 Kerr Effect

Source term arising from bound electrons in the medium could be expressed as[35]

$$\boldsymbol{S_{Kerr}}(\boldsymbol{r}, z, t) = \frac{4\pi}{c^2}\frac{\partial^2 \boldsymbol{P_{bound}(r,t)}}{\partial t^2} = \boldsymbol{S_{Kerr}}(\boldsymbol{r}, t) exp(i\psi(z,t)\hat{x}/2) + c.c \tag{2.6}$$

where $\hat{x}$ is the direction in x coordinate and the phase could be expressed as $\psi(z,t) = k_0 z - \omega_0 t$. Polarization field due to bound electrons is given by[1]

$$\boldsymbol{P_{bound}}(\boldsymbol{r}, t) = \chi_{NL} < \boldsymbol{E}.\boldsymbol{E} >_t \boldsymbol{E}(\boldsymbol{r}, t) \tag{2.7}$$

where χ_{NL} represents third order susceptibility of the medium. In order to approximate the refractive index, higher order harmonic terms are neglected. Therefore, with those assumptions, one could state that the refractive index could be expressed as the sum of linear and nonlinear components. Therefore, the refractive index could be given as[35]

$$n(r, \omega) = n_0(r, \omega) + n_2 I \tag{2.8}$$

where I is the average intensity of the pulse, n_0 is the linear refractive index and n_2 is the nonlinear refractive index. Therefore, substituting refractive index relation into the polarization field expression yields an equation that is given by[32]

$$\boldsymbol{P_{bound}}(\boldsymbol{r}, t) = \left(\frac{n_0}{4\pi}\right)^2 c n_2 |\epsilon(\boldsymbol{r}, t)|^2 \boldsymbol{E}(\boldsymbol{r}, t) \tag{2.9}$$

where $\epsilon(\boldsymbol{r},t)$ is the field amplitude and n_2 could be expressed as $n_2 = (8\pi^2/n_0^2 c)\chi_{NL}$ and intensity $I(\boldsymbol{r},t) = (c/4\pi)n_0 < \boldsymbol{E}.\boldsymbol{E} >_t = cn_0|\epsilon|^2/8\pi$. Therefore, substituting polarization field expression into source expression that yields Kerr effect source term could be given by[35]

$$\boldsymbol{S_{Kerr}}(\boldsymbol{r},z,t) = \frac{\omega_0^2 n_0^2 n_2}{4\pi c}|\boldsymbol{\epsilon}(\boldsymbol{r},z,t)|^2\boldsymbol{\epsilon}(\boldsymbol{r},z,t) \tag{2.10}$$

where n_2 is the electron contribution to the non-linear index. Furthermore $|\boldsymbol{\epsilon}|^2$ is calculated with $|\boldsymbol{\epsilon}|^2 = \boldsymbol{\epsilon}^*\boldsymbol{\epsilon}$ where $\boldsymbol{\epsilon}^*$ is the complex conjugate of the field amplitude.

2.2.2.2 Raman Scattering

General source term arising from Raman scattering using the envelope relation is given by[35]

$$\boldsymbol{S_{Raman}}(\boldsymbol{r},z,t) = \frac{4\pi}{c^2}\frac{\partial^2 \boldsymbol{P_{Raman}(r,t)}}{\partial t^2} = \boldsymbol{S_{Raman}}(\boldsymbol{r},t)exp(i\psi(z,t)\hat{x}/2) + c.c \tag{2.11}$$

Assuming the molecules in the nonlinear medium have three level system that having energies W_1, W_2 and excited state W_3. One could state that that transitions from W_1 to W_2 is not allowed. Furthermore, in order to make this model consistent, energy levels should have a relation such that $W_3 >> W_2 - W_1$. Also, assuming this Raman process is non-resonant in order to have an empty excited state that has an energy W_3. Utilizing these assumptions, one could express the polarization field that could be given by[35]

$$P_{Raman} = \chi_L Q(t)\epsilon(\boldsymbol{r},t) \tag{2.12}$$

where χ_L is the linear susceptibility and $Q(t)$ is an oscillating function that could be determined from the system of differential equations that is given by[35]

$$\frac{\partial^2 Q}{\partial t^2} + (\omega_R^2 + \Gamma_2^2)Q + 2\Gamma_2\frac{\partial Q}{\partial t} = -\omega_R\frac{\Omega_R^2}{\Omega}W(t)\frac{|\epsilon(\boldsymbol{r},t)|^2}{\epsilon_0^2} \tag{2.13}$$

$$\frac{\partial W}{\partial t} = \frac{\Omega_R^2}{\omega_R\Omega}\frac{|\epsilon(\boldsymbol{r},t)|^2}{\epsilon_0^2}\left(\frac{\partial Q}{\partial t} + \Gamma_2 Q\right) - \Gamma_1(W - W_0) \tag{2.14}$$

where $\omega_R = \mu\epsilon_0/\hbar$ is the Rabi frequency μ is the dipole transition moment matrix element that is related to the transition to excited state. Keep in mind that ϵ_0 is not

the electrical permittivity, it is the peak field amplitude. Also, Γ_1 and Γ_2 are damping rates and W is the difference between normalized population densities between state one and state two. If all the molecules are in the ground state for that particular medium, $W_0 = -1$. If one assumes slow variation in polarization, Raman scattering source term with that slow variation could be given by [35]

$$\boldsymbol{S}_{Raman}(\boldsymbol{r}, z, t) = -4\pi\frac{\omega_0^2}{c^2}\chi_{\mathcal{L}}Q(t)\boldsymbol{\epsilon}(\boldsymbol{r}, z, t) \tag{2.15}$$

2.2.2.3 Plasma Source Term

Plasma source term, wakefield term and relativistic term are arising due to the free electrons in the nonlinear medium. Therefore, this total source term i.e S_{free} could be expressed as $S_{free} = (4\pi/c^2)\partial\boldsymbol{J}/\partial t$ which is also equal to $S_{free} = S_{plasma} + S_{wake} + S_{rel}$. The total current density obeys the continuity equation which is given by[35]

$$\frac{\partial \boldsymbol{J}}{\partial t} + \nu_e \boldsymbol{J} = \frac{\omega_p^2}{4\pi}\left(1 + \frac{\delta n_e}{n_e}\right)\boldsymbol{E}(\boldsymbol{r}, t) \tag{2.16}$$

where plasma frequency $\omega_p(\boldsymbol{r}, z, t) = \sqrt{4\pi q^2 n_e(\boldsymbol{r}, z, t)/m}$ where q is the charge of the electron, m is the mass of the electron, ν_e is the neutral-electron collision frequency and n_e is the plasma density in the medium and δn_e is the perturbation in electron number density due to plasma wakefield. Electric field caused by perturbation in electron number density satisfies the following relation that is given by [35]

$$\left(\frac{\partial^2}{\partial t^2} + c^2\boldsymbol{\nabla}\times\boldsymbol{\nabla}\times + \omega_p^2\right)\boldsymbol{E_w} = \frac{q}{4m}\frac{\omega_p^2}{\omega_0^2}\boldsymbol{\nabla}|\epsilon|^2 \tag{2.17}$$

Therefore, electron number density perturbation could be expressed as $\delta n_e = \boldsymbol{\nabla}.\boldsymbol{E_w}/4\pi q$. Transforming both electric field terms and source terms related to the free electrons in the envelope form yields the free electron source that is given by[35]

$$S_{free} = \frac{\omega_p^2}{c^2}\left(1 + \frac{\delta n_e}{n_e} - \frac{\delta m}{m}\right)\left(1 - i\frac{\nu_e}{\omega_0}\right)\epsilon(r, z, t) \tag{2.18}$$

Assuming a weakly relativistic limit, that is $|q\epsilon/mc\omega_0| << 1$, one could write the expression for perturbations of electron mass due to relativistic motion that is given by [35]

$$\frac{\delta m}{m} = \frac{1}{4}\left(\frac{q}{mc\omega_0}\right)^2|\epsilon|^2 \tag{2.19}$$

Therefore, separating the source term due to free electron motion is vital to find individual contributions of plasma term, relativistic term, and wakefield term. Therefore, separating Equation 2.18 yields plasma source term that is given by [35]

$$S_{plasma}(r,z,t) = \frac{\omega_p^2(r,z,t)}{c^2}\left(1 - i\frac{\nu_e}{\omega_0}\right)\epsilon(r,z,t) \tag{2.20}$$

2.2.2.4 Wakefield Term

Separating Equation 2.18 yields wakefield term that is given by[35]

$$\boldsymbol{S}_{wake}(\boldsymbol{r},z,t) = \frac{\omega_p(\boldsymbol{r},z,t)^2}{c^2}\frac{\delta n_e}{n_e}\boldsymbol{\epsilon}(\boldsymbol{r},z,t) \tag{2.21}$$

where δn_e is the plasma number density perturbation[32, 35].

2.2.2.5 Relativistic Term

Separating Equation 2.18 yields relativistic term that is given by[35]

$$S_{rel}(r,z,t) = -\frac{\omega_p^2(r,z,t)}{4c^2}\left(\frac{q|\epsilon(r,z,t)|^2}{mc\omega_0}\right)^2\epsilon(r,z,t) \tag{2.22}$$

This term is needed for critical self-focusing power due to plasma [6, 31]

2.2.2.6 Ionization term

Energy depletion due to ionization could be expressed as[35]

$$\frac{\partial W_f}{\partial t} = U_{ion}\int n_e(r,z,\tau)d\sigma \tag{2.23}$$

where U_{ion} is the ionization energy of the respective medium. For example, for air it is $U_{air} = 0.2U_{O_2} + 0.8U_{N_2}$. W_f is the total field energy and σ refers to cross-sectional area. Therefore, W_f could be rewritten as the following expression that is given by[35]

$$W_f = -\int d\sigma \int d(c\tau) < \boldsymbol{E}.\boldsymbol{E} >_t /4\pi \tag{2.24}$$

where $< \boldsymbol{E}.\boldsymbol{E} >_t = |\epsilon|^2/2$. Therefore, one could substitute the integral form of the energy to the differential form yields[35]

$$\frac{\partial|\epsilon|^2}{\partial z} = -8\pi U_{ion}\frac{\partial n_e}{c\partial\tau} \tag{2.25}$$

It could be stated that field energy loss due to ionization from the above equation. Furthermore, the source term for this energy depletion due to ionization is given by [35]

$$\boldsymbol{S}_{ion}(\boldsymbol{r}, z, t) = -8\pi i k_0 \frac{U_{ion}}{c|\boldsymbol{\epsilon}(\boldsymbol{r}, \boldsymbol{z}, \boldsymbol{t})|^2} \frac{\partial n_e}{\partial t} \boldsymbol{\epsilon}(\boldsymbol{r}, z, t) \tag{2.26}$$

Ionization term is specifically essential for the pulses that are highly energetic enough to ionize the medium[35]. Since energy has to be conserved, while ionization there needs to be a power-loss due to ionization.

Therefore, using all the source terms would yield the full nonlinear propagation equation. In this study, Raman effect, wakefield, and relativistic terms are excluded in the propagation equation.

2.3 Propagation Equation for Ionizing Short Laser Pulses

Using the linear source terms, ionization term, Kerr effect, and plasma source term would give the general propagation equation[9, 10, 46]. Note that electron-neutral collision frequency has taken to be zero. Therefore, the propagation equation used in this study is given by[11, 35]

$$\left(\nabla_\perp^2 + 2ik_0\frac{\partial}{\partial z} + k_0\beta_2\frac{\partial^2}{\partial \tau^2} + \frac{\omega_0^2 n_0^2 n_2}{4\pi c}|\epsilon(r,z,\tau)|^2 - \frac{\frac{4\pi q^2 n_e(r,z,\tau)}{m}}{c^2} + \frac{8\pi i k_0}{c}\frac{U_{ion}}{|\epsilon(r,z,\tau)|^2}\frac{\partial n_e}{\partial \tau}\right)\epsilon(r,z,\tau) = 0 \tag{2.27}$$

2.4 Propagation Equation for Non-Ionizing Short Laser Pulses

For non-ionizing lasers, plasma and ionization terms would be excluded in the propagation equation. Also, plasma and ionization terms contribute so little to the propagation equation if the laser power is not sufficient enough to ionize the medium. That means, while propagating in space in low power, both equations with ionization

and equation without ionization should behave similarly. Therefore we may compare those equations in low intensity propagation regime (LIPR)[41, 42, 43]. Hence, propagation equation for non-ionizing pulse is given by[35, 42]

$$\left(\nabla_{\perp}^{2} + 2ik_0\frac{\partial}{\partial z} + k_0\beta_2\frac{\partial^2}{\partial\tau^2} + \frac{\omega_0^2 n_0^2 n_2}{4\pi c}|\epsilon(r,z,\tau)|^2\right)\epsilon(r,z,\tau) = 0 \tag{2.28}$$

2.5 Non Linear Schrödinger Equation

A typical non-linear Schrödinger equation could be described as[5, 7]

$$i\frac{\partial u}{\partial \xi} + \frac{1}{2}\frac{\partial^2 u}{\partial \tau^2} + |u|^2 u = -i\kappa|u|^2 u \tag{2.29}$$

where ξ is a space coordinate and τ is time (proper or plain time).
As could be seen above, there are some missing terms in this non-linear Schrödinger equation in order to be similar to the propagation equation stated in this study. In order to make both equations similar, there need to be additional terms in the non-linear Schrödinger equation. If those terms would be added, it is called "Extended non-linear Schrödinger equation".
After adding those terms, both propagation equation that has been declared earlier and extended nonlinear Schrödinger equations behave similarly. Therefore, solving techniques for extended non-linear Schrödinger equations are highly applicable to the propagation equation in this study.

2.6 Methods For Solving Propagation Equation

It may be said there are four best candidates to solve extended non-linear Schrödinger type equations. These could be named as follows.

- Variational approach[2, 3, 43]
- Method of undetermined coefficients[33, 35]
- Source dependent expansion method[1, 36]
- Split-Step Fourier Method[23, 11]

in this study, the method of unknown coefficients and split-step Fourier method would be used in order to solve the propagation equation.

2.6.1 Variational Approach

The variational method basically approaches the problem as a Lagrangian mechanic and treat the solutions to be as an equation of motion. Therefore there need to be two separate expressions for both linear and non-linear part of the problem. These expressions are given by [2, 7]

$$\frac{\partial}{\partial z}\frac{\partial L_c}{\partial\left(\frac{\partial \epsilon_i}{\partial z}\right)}+\frac{\partial}{\partial \tau}\frac{\partial L_c}{\partial\left(\frac{\partial \epsilon_i}{\partial \tau}\right)}-\frac{\partial L_c}{\partial \epsilon_i}=Q_i \tag{2.30}$$

where i is the index for field amplitude that ranges from 1-2. With $i = 2$, field amplitude becomes $\epsilon_2 = \epsilon^*$ *i.e* becomes the complex conjugate of the field amplitude. Here, Q represents the non-linear processes that are described as follows[7]

$$Q_i=\frac{\partial L_{nc}}{\partial \epsilon_i}-\frac{\partial}{\partial z}\frac{\partial L_{nc}}{\partial\left(\frac{\partial \epsilon_i}{\partial z}\right)}-\frac{\partial}{\partial \tau}\frac{\partial L_{nc}}{\partial\left(\frac{\partial \epsilon_i}{\partial \tau}\right)}. \tag{2.31}$$

Therefore, one can determine the Lagrangian for a specific propagation equation and solve the system of the differential equations in order to obtain the equations of motion for this system in terms of the unknown coefficients.

2.6.2 Method of Undetermined Coefficients

The method of undetermined coefficients could be utilized by inserting the field amplitude into the propagation equation. One could rearrange the terms in such a way that there are some coefficients for spatial coordinates and time. Since spatial coordinates and time equals zero gives the obvious solution, coefficients of the coordinates have to be zero in order to satisfy the propagation equation[26, 35].

One trick to obtain the propagation equation with inserted field amplitude solution in the form of powers of spatial coordinates and time is to multiply the equation with the absolute value square of the field amplitude and divide by the complex conjugate of the field amplitude. By utilizing this method, one may obtain an equation with

no exponential term that arising from the field amplitude. However, there are still exponential terms arising from the number density term. An approximation for this exponential is to make a Taylor series expansion for that exponential in order to have an equation in the form of powers of spatial coordinates and time, *i.e* (r, τ). The resulting equation would yield 6 equations if one equates the total equation with respect to their like-powers, which is utilizing the method of undetermined coefficients. However, there are 7 unknowns with 6 equations arising from the method of undetermined coefficients. Therefore, the seventh equation has to come from an external identity, that is given by [35]

$$\frac{\partial n_e}{\partial \tau} = \frac{2\pi\omega_0}{(\kappa-1)!} exp\left(-\frac{2\kappa r^2}{R(z)^2} - \frac{2\kappa\tau^2}{T(z)^2}\right)\left(\frac{I(z)}{I_{mp}}\right)^{\kappa} n_n \tag{2.32}$$

where κ is the multiphoton ionization constant, n_n is the neutral density in the medium and $I(z)$ is the intensity of the wave that is defined by $I(z) = \frac{2P(z)}{\pi R^2(z)}$. This identity first arises from an approximation which is given by [35]

$$\frac{\partial n_e}{\partial t} = W n_n - \eta n_e - \beta_r n_e^2 \tag{2.33}$$

where W is the photoionization rate, η is the electron-attachment rate coefficient and β_r is the recombination coefficient. For the pulses which have durations $\approx$ 1 psecs or less, electron-electron attachment and recombination coefficients could be excluded from the expression[18, 35].

Using the multiphoton ionization for photoionization rate would also yield an expression for W that is given by [35]

$$W_{mp} = \frac{2\pi\omega_0}{(\kappa-1)!}\left(\frac{I(z)}{I_{mp}}\right)^{\kappa} \tag{2.34}$$

Although method of undetermined coefficients is not the most elegant way to obtain the unknown coefficients *i.e* $R(z), T(z), \alpha(z), \beta(z), P(z)$ and $\phi(z)$, it would result in an good approximation for their behavior while propagating.

As stated before, utilizing the method of undetermined coefficients requires the substitution of field amplitude to the propagation equation. Therefore, applying this step yields a very long expression given below.

$$
\begin{aligned}
&32P(z)\sqrt{\frac{P(z)}{cn_0R(z)^2}}\\
&\frac{\exp\left(-\frac{2r^2(1+i\alpha(z))}{R(z)^2}-\frac{r^2(1-i\alpha(z))}{R(z)^2}-\frac{2\tau^2(1+i\beta(z))}{T(z)^2}-\frac{\tau^2(1-i\beta(z))}{T(z)^2}+i\phi(z)\right)}{P_{\mathrm{NL}}R(z)^2}\\
&-\frac{ic2^{\kappa-2}\pi^{-\kappa}n_0\lambda_{\mathrm{MPI}}R(z)^2\left(\frac{P(z)}{R(z)^2}\right)^{\kappa}\sqrt{\frac{P(z)}{cn_0R(z)^2}}\exp\left(\frac{r^2(1-i\alpha(z))}{R(z)^2}+\frac{\tau^2(1-i\beta(z))}{T(z)^2}+i\phi(z)\right)}{P(z)}\\
&+\frac{16r^3(1+i\alpha(z))^2\sqrt{\frac{P(z)}{cn_0R(z)^2}}\exp\left(-\frac{r^2(1+i\alpha(z))}{R(z)^2}-\frac{\tau^2(1+i\beta(z))}{T(z)^2}+i\phi(z)\right)}{rR(z)^4}-\\
&\frac{16r(1+i\alpha(z))\sqrt{\frac{P(z)}{cn_0R(z)^2}}\exp\left(-\frac{r^2(1+i\alpha(z))}{R(z)^2}-\frac{\tau^2(1+i\beta(z))}{T(z)^2}+i\phi(z)\right)}{rR(z)^2}-\\
&\beta_2k_0\left(\frac{16\tau^2(1+i\beta(z))^2\sqrt{\frac{P(z)}{cn_0R(z)^2}}\exp\left(-\frac{r^2(1+i\alpha(z))}{R(z)^2}-\frac{\tau^2(1+i\beta(z))}{T(z)^2}+i\phi(z)\right)}{T(z)^4}-\right.\\
&\left.\frac{8(1+i\beta(z))\sqrt{\frac{P(z)}{cn_0R(z)^2}}\exp\left(-\frac{r^2(1+i\alpha(z))}{R(z)^2}-\frac{\tau^2(1+i\beta(z))}{T(z)^2}+i\phi(z)\right)}{T(z)^2}\right)+\\
&256\pi q^2P(z)n_e(z)\sqrt{\frac{P(z)}{cn_0R(z)^2}}\\
&\frac{\exp\left(-\frac{2r^2(1+i\alpha(z))}{R(z)^2}-\frac{r^2(1-i\alpha(z))}{R(z)^2}-\frac{2\kappa r^2}{R(z)^2}-\frac{2\tau^2(1+i\beta(z))}{T(z)^2}-\frac{\tau^2(1-i\beta(z))}{T(z)^2}-\frac{2\kappa\tau^2}{T(z)^2}+i\phi(z)\right)}{c^3mn_0\omega_0^2R(z)^2}\\
&+2ik_0\left(\frac{2\left(\frac{P'(z)}{cn_0R(z)^2}-\frac{2P(z)R'(z)}{cn_0R(z)^3}\right)\exp\left(-\frac{r^2(1+i\alpha(z))}{R(z)^2}-\frac{\tau^2(1+i\beta(z))}{T(z)^2}+i\phi(z)\right)}{\sqrt{\frac{P(z)}{cn_0R(z)^2}}}+\right.\\
&4\sqrt{\frac{P(z)}{cn_0R(z)^2}}\exp\left(-\frac{r^2(1+i\alpha(z))}{R(z)^2}-\frac{\tau^2(1+i\beta(z))}{T(z)^2}+i\phi(z)\right)\times\\
&\left(\frac{2r^2(1+i\alpha(z))R'(z)}{R(z)^3}-\frac{ir^2\alpha'(z)}{R(z)^2}\right.\\
&\left.\left.+\frac{2\tau^2(1+i\beta(z))T'(z)}{T(z)^3}-\frac{i\tau^2\beta'(z)}{T(z)^2}+i\phi'(z)\right)\right)=0 \quad (2.35)
\end{aligned}
$$

Although it is possible to apply the method of undetermined coefficients to Equation 2.35 after using Taylor series to the exponential terms in the equation, one could simplify the equation by multiplying it with the absolute value square of the field amplitude and divide by the field amplitude complex conjugate. Hence applying this

to the propagation equation yields a more simple equation that is given by

$$\frac{64\pi q^2 P(z) n_e(z) e^{-2(\kappa+1)\left(\frac{r^2}{R(z)^2}+\frac{\tau^2}{T(z)^2}\right)}}{c^3 m n_0 \omega_0^2 R(z)^2} - ic2^{\kappa-4}\pi^{-\kappa} n_0 \lambda_{\text{MPI}} \left(\frac{P(z)}{R(z)^2}\right)^{\kappa-1} \times e^{\frac{2r^2}{R(z)^2}+\frac{2\tau^2}{T(z)^2}} + \frac{ik_0 P'(z)}{P(z)} - \frac{4k_0 r^2 \alpha(z) R'(z)}{R(z)^3} + \frac{4ik_0 r^2 R'(z)}{R(z)^3} + \frac{2k_0 r^2 \alpha'(z)}{R(z)^2} - \frac{2ik_0 R'(z)}{R(z)} - \frac{4k_0 \tau^2 \beta(z) T'(z)}{T(z)^3} + \frac{4ik_0 \tau^2 T'(z)}{T(z)^3} + \frac{2k_0 \tau^2 \beta'(z)}{T(z)^2} + \frac{4\beta_2 k_0 \tau^2 \beta(z)^2}{T(z)^4} - \frac{4\beta_2 k_0 \tau^2}{T(z)^4} - \frac{8i\beta_2 k_0 \tau^2 \beta(z)}{T(z)^4} + \frac{2i\beta_2 k_0 \beta(z)}{T(z)^2} + \frac{2\beta_2 k_0}{T(z)^2} - 2k_0\phi'(z) + \frac{8P(z)e^{-\frac{2r^2}{R(z)^2}-\frac{2\tau^2}{T(z)^2}}}{P_{\text{NL}} R(z)^2} + \frac{8ir^2\alpha(z)}{R(z)^4} - \frac{4r^2\alpha(z)^2}{R(z)^4} + \frac{4r^2}{R(z)^4} - \frac{4i\alpha(z)}{R(z)^2} - \frac{4}{R(z)^2} = 0 \tag{2.36}$$

After this step, one could expand the exponential terms in Equation 2.36 with Taylor series until $\mathcal{O}(3)$ and separate the Equation 2.36 to real and imaginary parts. Separately equating the like-powers of real and imaginary parts yields the differential equations needed for to solve the system. Hence, the equations that arising from real parts are given by

$$\frac{64\pi q^2 P(z) n_e(z)}{c^3 m n_0 \omega_0^2 R(z)^2} + \frac{2\beta_2 k_0}{T(z)^2} - 2k_0\phi'(z) + \frac{8P(z)}{P_{\text{NL}} R(z)^2} - \frac{4}{R(z)^2} = 0 \tag{2.37}$$

$$-\frac{128\pi(\kappa+1)q^2 P(z) n_e(z)}{c^3 m n_0 \omega_0^2 R(z)^2 T(z)^2} - \frac{4k_0\beta(z)T'(z)}{T(z)^3} + \frac{2k_0\beta'(z)}{T(z)^2} + \frac{4\beta_2 k_0 \beta(z)^2}{T(z)^4} - \frac{4\beta_2 k_0}{T(z)^4} - \frac{16P(z)}{P_{\text{NL}} R(z)^2 T(z)^2} = 0 \tag{2.38}$$

$$-\frac{128\pi(\kappa+1)q^2 P(z) n_e(z)}{c^3 m n_0 \omega_0^2 R(z)^4} - \frac{4k_0\alpha(z)R'(z)}{R(z)^3} + \frac{2k_0\alpha'(z)}{R(z)^2} - \frac{16P(z)}{P_{\text{NL}} R(z)^4} - \frac{4\alpha(z)^2}{R(z)^4} + \frac{4}{R(z)^4} = 0 \tag{2.39}$$

Equations that arising from the imaginary parts are also given by

$$c\left(-2^{\kappa-4}\right)\pi^{-\kappa} n_0 \lambda_{\text{MPI}} \left(\frac{P(z)}{R(z)^2}\right)^{\kappa-1} + \frac{k_0 P'(z)}{P(z)} - \frac{2k_0 R'(z)}{R(z)} + \frac{2\beta_2 k_0 \beta(z)}{T(z)^2} - \frac{4\alpha(z)}{R(z)^2} = 0 \tag{2.40}$$

$$-\frac{c2^{\kappa-3}\pi^{-\kappa}n_0\lambda_{\text{MPI}}\left(\frac{P(z)}{R(z)^2}\right)^{\kappa-1}}{T(z)^2}+\frac{4k_0T'(z)}{T(z)^3}-\frac{8\beta_2k_0\beta(z)}{T(z)^4}=0 \quad (2.41)$$

$$-\frac{c2^{\kappa-3}\pi^{-\kappa}n_0\lambda_{\text{MPI}}\left(\frac{P(z)}{R(z)^2}\right)^{\kappa-1}}{R(z)^2}+\frac{4k_0R'(z)}{R(z)^3}+\frac{8\alpha(z)}{R(z)^4}=0 \quad (2.42)$$

Where $\lambda_{MPI} = 8\pi k_0 U_{ion}/cI_{mp}^{\kappa}$ used for simplification in the equations. One could state that from Equation [2.37 - 2.42] are six equations. However, there are seven unknowns, i.e, $R(z), T(z), P(z), n_e(z), \alpha(z), \beta(z)$ and $\phi(z)$. Therefore, there needs to be a seventh equation in order to solve this system of differential equations. The seventh equation is the number density relation, *i.e*, Equation 2.32

Expectations from the method of undetermined coefficient solution are to behave similarly to the solution without ionization problem in the low intensity propagation regime since electron number density is not sufficient to affect the overall behavior of the pulse. However, in the high intensity propagation regime, one could expect that the energy has to decrease because of the ionization in the medium. Furthermore, the power of the pulse has to decrease because of the same phenomenon.

2.6.3 Source Dependent Expansion Method

In source dependent expansion, characteristics of the modes are governed by the driving current density and treat the input wave as complex amplitude, curvature, and waist[36]. Although the input field amplitude structure is very similar to the field amplitude expression that has been expressed at the beginning of this thesis, the main difference is there is no chirping term referenced explicitly since the curvature term is a function of proper time and includes the information from the chirp itself.

The field amplitude to start for source dependant expansion is given by[36]

$$\epsilon(r,z,\tau) = B(z,\tau)exp\left(i\phi(z,\tau)-\frac{(1+i\alpha(z,\tau))r^2}{R^2(z,\tau)}\right) \quad (2.43)$$

where $B(z,\tau)$ is the field amplitude. The procedure itself is too long to include in this study and since this method would not be applied, it is more convenient to express the

ending results of the propagated wave. Therefore, the equations of motion are given by[35, 34, 33]

$$\frac{1}{BR}\frac{\partial(BR)}{\partial z} = F_i \tag{2.44}$$

$$\frac{\partial\phi}{\partial z} + \frac{(1+\alpha^2)}{k_0 R^2} + \frac{\alpha}{R}\frac{\partial R}{\partial z} - \frac{1}{2}\frac{\partial\alpha}{\partial z} = -F_r \tag{2.45}$$

$$\frac{1}{R}\frac{\partial R}{\partial z} + \frac{2\alpha}{k_0 R^2} = -G_i \tag{2.46}$$

$$\frac{1}{2}\frac{\partial\alpha}{\partial z} + \frac{(1+\alpha^2)}{k_0 R^2} = -G_r - \alpha G_i \tag{2.47}$$

Where F and G are complex functions in source dependant expansion method and i and r are the real and imaginary parts of those functions. F and G could be defined as [36, 35]

$$F(z,\tau) = \frac{1}{2k_0}\int_0^\infty d(2r^2/R^2)M(r,z,\tau)exp(-2r^2/R^2) \tag{2.48}$$

$$G(z,\tau) = \frac{1}{2k_0}\int_0^\infty d(2r^2/R^2)M(r,z,\tau)exp(-2r^2/R^2)(1-2r^2/R^2) \tag{2.49}$$

where $M(r,z,\tau)$ is the non-linear part of the propagation equation.

2.6.4 Split-Step Fourier Method

Split-step Fourier method is one of the numerical methods that could evaluate the propagation equation that is one of the pseudo-spectral methods[1].

Split-step could be defined for a propagation equation in the form of as shown as below equation[23]

$$\frac{\partial\epsilon(r,z,t)}{\partial z} = \left(\hat{\mathcal{L}} + \hat{\mathcal{N}}\right)\epsilon(r,z,t) \tag{2.50}$$

where $\hat{\mathcal{N}}$ is the non-linear part of the propagation equation and $\hat{\mathcal{L}}$ is the linear part of the propagation equation. As could be seen, linear and non-linear parts of the equations are still in the operator form.

Therefore, split-step method could be expressed as[1, 23]

$$\epsilon(r,z+h,t) = exp\left(h(\hat{\mathcal{L}} + \hat{\mathcal{N}})\right)\epsilon(r,z,t) \tag{2.51}$$

where h is the step size along z-direction. In order to be more centralized, one could rearrange the expression in such a way that[23]

$$\epsilon(r, z+h, t) = exp\left(h\frac{\hat{\mathcal{L}}}{2}\right) exp\left(h\hat{\mathcal{N}}\right) exp\left(h\frac{\hat{\mathcal{L}}}{2}\right) \epsilon(r, z, t) \tag{2.52}$$

Keeping in mind that this part only represents the split-step method. Plain split-step would just work fine without the Fourier method addition. Also, without Fourier addition, it is not a pseudo-spectral method. However, the plain split-step method needs a symbolic calculation tool such as $Mathematica^{TM}$ or a Python module named as SymPy. Using these tools are effective, yet have very slow computation time since these tools would try to calculate the respective derivatives numerically and turn back to symbolic form. Therefore, imposing split-step Fourier method reflects the whole problem into a numeric calculation by transforming the respective derivatives into their angular velocity form.

For example, using split-step Fourier method on Equation(1.17) could be given as[23]

$$f_1 = \mathcal{F}^{-1}\left(exp\left(\frac{h}{2}\mathcal{F}(\hat{\mathcal{L}})\right)\mathcal{F}\left(\epsilon(r, z, t)\right)\right) \tag{2.53}$$

where $\mathcal{F}$ and $\mathcal{F}^{-1}$ denotes the Fourier transform and inverse Fourier transform respectively.

One could utilize the Fourier transform application into the whole propagation equation. Hence, split-step Fourier method for the first half of the expression is

$$f_2 = exp\left(f_1 h\mathcal{F}(\hat{\mathcal{N}})\right) \tag{2.54}$$

Finally, whole equation is

$$\epsilon(r, z+h, t) = \mathcal{F}^{-1}(\mathcal{F}(f_2)f_1) \tag{2.55}$$

Simulations for such a problem could be done by any numerical solver such as Python with NumPy, R, or Matlab. In this study, all the simulations are done within the Python environment.

2.7 Propagation Equation without Ionization

It could be deduced that the propagation equation without ionization and with ionization should behave similarly in the low intensity propagation regime since the intensity required to ionize the region is not sufficient enough. Therefore, some parameters such as plasma density could be approximated near the high intensity propagation regime.

The propagation equation without ionization could be derived by excluding the plasma terms from the propagation equation with ionization. Keep in mind that plasma terms are not the only non-linear term in the expression but also Kerr effect contributes to the non-linear effects too. Hence, the propagation equation reduces to[35, 43]

$$\left(\nabla_{\perp}^{2} + 2ik_0\frac{\partial}{\partial z} + k_0\beta_2\frac{\partial^2}{\partial \tau^2} + \frac{\omega_0^2 n_0^2 n_2}{4\pi c}|\epsilon(r,z,\tau)|^2\right)\epsilon(r,z,\tau) = 0 \tag{2.56}$$

Solving this equation with the method of variation would yield the results in terms of R, T, P, α, β. Hence those differential equations are given by[41, 42, 43]

$$\frac{d(PT)}{dz} = 0 \tag{2.57}$$

$$\alpha = -\frac{k_0 R}{2}\frac{dR}{dz} \tag{2.58}$$

$$\beta = \frac{T}{2\beta_2}\frac{dT}{dz} \tag{2.59}$$

$$\frac{d^2R}{dz^2} - \frac{4}{k_0^2 R^3}\left(1 - \frac{P}{P_{CR}}\right) = 0 \tag{2.60}$$

$$\frac{d^2T}{dz^2} - \frac{4\beta_2^2}{T^3} - \frac{4\beta_2 P}{k_0 R^2 T P_{CR}} = 0 \tag{2.61}$$

Hence, one could solve this system of differential equations in order to indicate the behavior of the pulse in the non-linear medium without taking plasma generation into account.

Following figures are initialized with $T_0 = 0.66\times10^{-12}s$, $R_0 = 1cm$,$P_0 = \lambda_0^2/2\pi n_0 n_2$, $\alpha_0 = 0.5$,$\beta_0 = -20$, $\lambda_0 = 0.775 \times 10^{-4}cm$, $\beta_2 = 2.2 \times 10^{-31}$, $n_2 = 3 \times 10^{-19}$

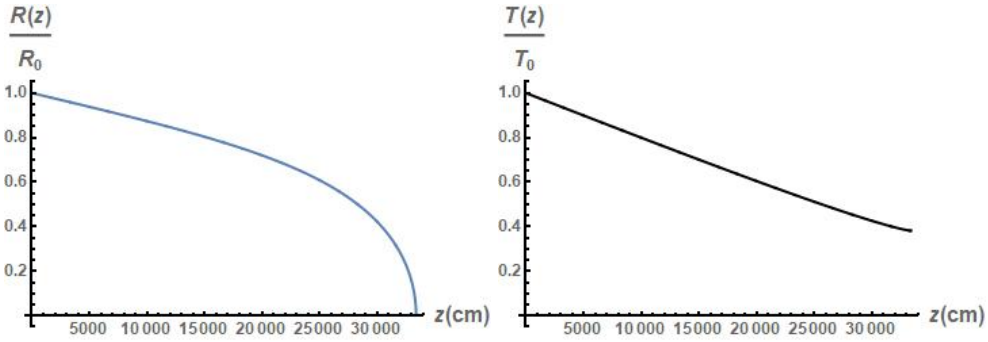

(a) Spot Size vs. propagation distance

(b) Pulse Length vs. propagation distance

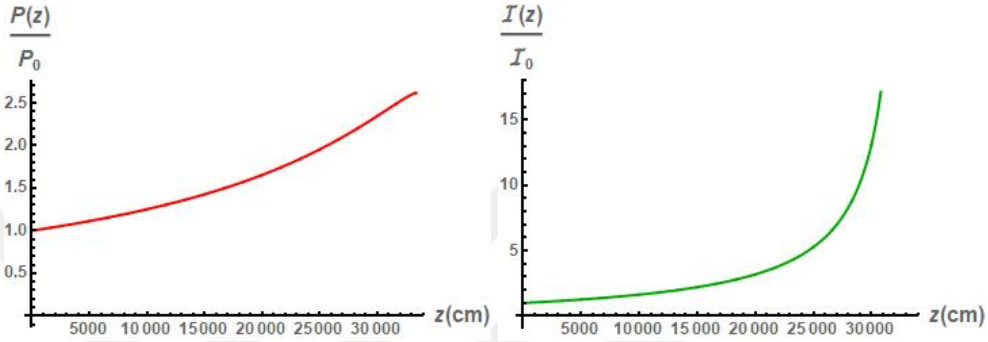

(c) Power vs. propagation distance

(d) Intensity vs. propagation distance

Figure 2.1: Wave parameters vs. propagation distance indicating the evolution of the pulse while propagating in the non-linear medium.

As could be seen above, the spot size gets smaller while the power and intensity of the pulse become larger. Near high intensity propagation regime, intensity reaches up to $\approx 300I_0$ which is sufficient to ionize the medium. These values have not been shown on the graph because $\times 300$ makes it unable to read the graph in the low intensity propagation regime. At the beginning of the propagation initial intensity is in the order of $\approx 10^9 W/cm^2$

In the *Chapter 3*, results arising from the propagation equation with the plasma generation and propagation equation without plasma generation would be compared in terms of their evolution and their behavior in low intensity propagation regime which would have to be similar

CHAPTER 3

SIMULATION RESULTS IN ATMOSPHERE AND DISCUSSION

In this section, results arising from split-step Fourier method and method of undetermined coefficients would be given. Their simulations would be presented. These simulations would be discussed deeply in terms of their behavior.

Figures in this chapter are initialized with the following relations unless it is stated otherwise.

Table 3.1: Initials

P_0=$\lambda_0^2/2\pi n_0 n_2$	T_0=$0.66 \times 10^{-12} s$	R_0=$1cm$
n_{atm}=$2.5 \times 10^{19} p/cm^3$	β_0=-20	β_2=$2.2 \times 10^{-}31 s^2/cm$
α_0=0.5	λ_0=$0.775 \times 10^{-4} cm$	n_0=1
n_2=3×10^{-19}	k_0= $2\pi/\lambda_0$	ω_0= ck_0/n_0
κ=8	U_{ion}=$14.35eV$	I_{mp}=$5.6 \times 10^{13} W/cm^2$

3.1 Simulations of Split-Step Fourier Method

Split-step Fourier method was explained in detail in the *Chapter 1*. Utilizing this method requires a numerical solver such as Matlab, Python or any other preferable solver. In this thesis, Python was used to solve this system with the specifications given below for reproducibility.

Python version: 3.6.8	NumPy version: 1.17	Plotly version: 4.12

Furthermore, source code for this Python project could be found in the *Appendix A*.

3.1.1 Simulations for Field Amplitude Evolution with SSFM

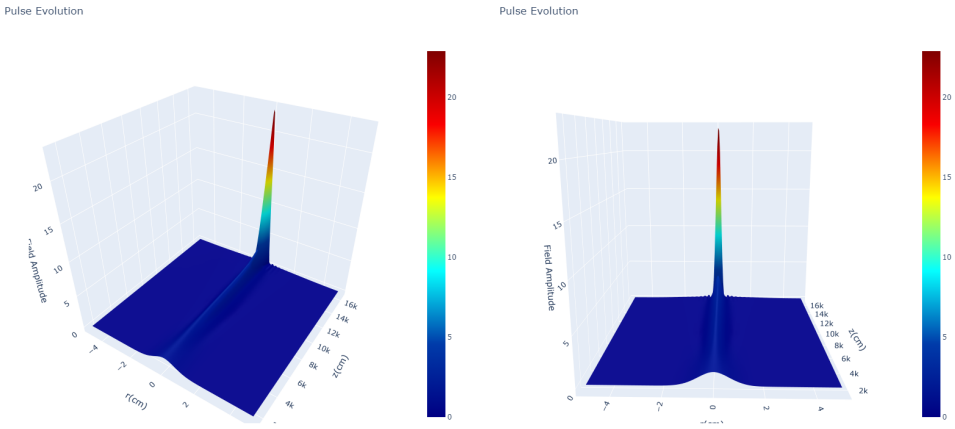

(a) Field Amplitude vs. propagation distance and radius

(b) Field Amplitude vs. propagation distance and radius(different angle)

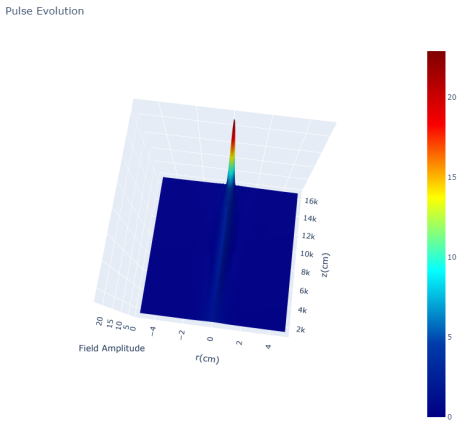

(c) Field Amplitude vs. propagation distance and radius(different angle)

Figure 3.1: Field amplitude vs. propagation distance indicating the evolution of the pulse while propagating in the non-linear medium.

As could be expected from the behavior of the propagation equation without ionization, Figure 3.1 indicates that pulse starts to focus and intensity reaches to a critical point where medium starts to ionize. However, the main difference with this solution and with the one without ionization is the place where pulse is focused. In this

solution, pulse has focused on where $z \approx 165m$ but in the pulse without ionization solution it has focused at a distance where $z \approx 330m$. This different was expected since the ionization terms in the propagation equation contributes to the field amplitude derivative with respect to propagation distance and make it higher. Therefore this much of a difference between propagation distance would be expected. Furthermore, since radius would decrease the value of field amplitude in the first place, it could be seen again that this focusing happens only in a small region where radius lies between in a range $r \longrightarrow -0.2cm$ to $0.2cm$ region.

This figure includes both low intensity propagation regime and high intensity propagation regime(where z is close to 150 meters). However it is not easy to see the evolution in the high intensity propagation regime only from this figure. Hence, below figure expresses it more clearly where the propagation distance lies between $z \approx 150m$

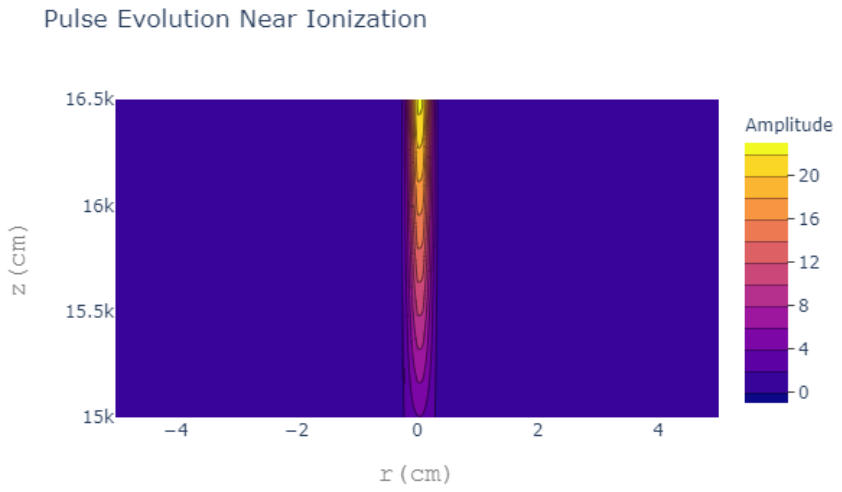

Figure 3.2: Field amplitude vs. propagation distance near ionization.

As could be seen more clearly from the Figure 3.2 field amplitude is getting larger in the high intensity propagation regime and this is an excellent indicator that pulse would ionize the region. Keep in mind that this simulations does not include the post-ionization region. Therefore, it is not possible to determine what is the evolution near post-ionization. Furthermore, as one could see from the figures, this iterative process of split-step Fourier method would done with the step size of $h = 15m$. This step

size has chosen because the computational difficulty to handle such a long iteration is time consuming and yielding nearly the same results. If one inspects Figure 3.1 and Figure 3.2 in detail, expecting an increase in the electron number density in the medium is inevitable since field amplitude and electron number density are directly related to each other. However, this relation of number density and field amplitude is not linearly. Therefore, one should expect a sharp increase in the region of self-focusing effects become more important.

3.1.2 Simulations for Number Density Evolution with SSFM

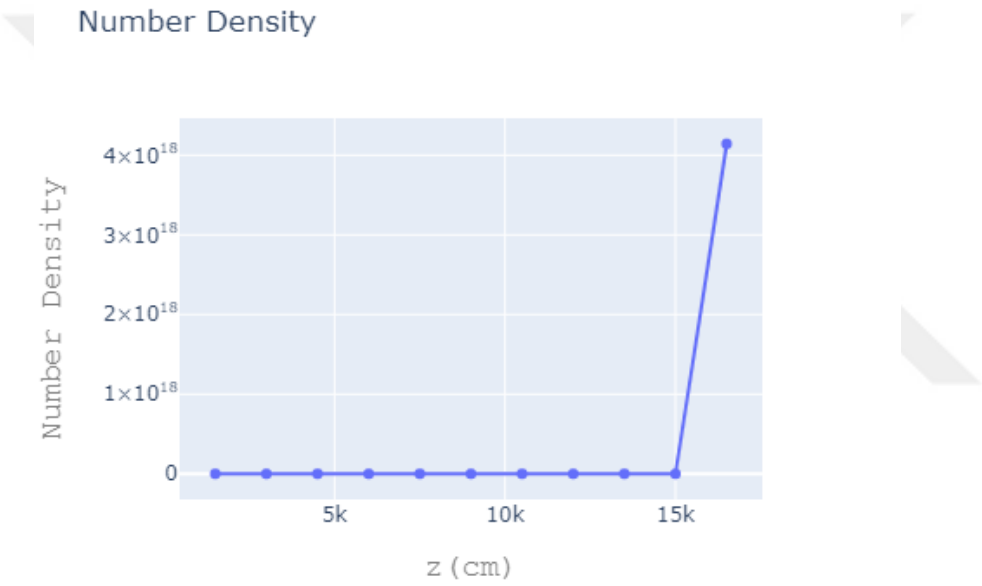

Figure 3.3: Number density at $r = 0$ vs. propagation distance

As could be seen in the Figure 3.3, at the last step size, number density reaches to an order of $10^{18} particles/cm^3$. At the other points it is not completely zero but not in a limit that figure could show. It is in a region where $10^2 - 10^{10} particles/cm^3$. One could state that at the order of $10^{18} particles/cm^3$, medium is not fully ionized since $\frac{n(z)}{n_{atm}} \approx 0.2$ in this region. Therefore, pulse become fully focused at a region where propagation distance is a little bit larger than $z = 165m$, approximately at $z = 167m - 170m$. In order to achieve that accuracy, step size must be reduced to

an order such as $h \approx 5m$ and it is stated that small step size leads to a computational difficulty and sometimes small errors that never occur in larger step size such as gradient overflow. Differences with full ionization and partial ionization would be discussed deeply in the section of method of undetermined coefficient simulations and similarity of both models will be discussed. As explained before, relation between electron number density and field amplitude are not linear. Therefore, one could expect a small increase in the region of small field amplitude increase and a dramatic increase in electron number density where field amplitude change is larger. In the region where self-focusing makes field amplitude larger, sharper increase in the electron number density had been expected and Figure 3.3 indicates that behavior explicitly and clearly. Even if initial self-focusing parameter α_0 was negative, similar behavior in the region where field amplitude becomes larger would be seen in the electron number density with a considerably longer distance of self-focusing.

3.2 Simulations of Method of Undetermined Coefficients

The most important subject to mention is the error that arising from Taylor expansion of the exponential term related to number density. Since only two terms of the Taylor expansion have been used in order to equate the like powers, there is an error in the order of $\mathcal{O}(3)$. One can reduce the error by expanding the exponential term further. However, radius and proper time terms in the order of r^3, r^4, r^5 *etc.* would yield new equations without having useful information in it. Therefore, as Sprangle stated, it is not the most elegant way to solve this problem.[35]. Despite all the stated error prone for method of undetermined coefficients, issues due to step size in split step Fourier method do not applicable for method of undetermined coefficients. Since only requirement to utilize method of undetermined coefficients is to solve the system of differential equations with a differential equation solver like $Mathematica^{TM}$, obtaining solutions with more resolution is possible. However, utilizing method of undetermined coefficients requires more tedious work if one compares split step Fourier method and method of undetermined coefficients.

3.2.1 Simulations for Spot Size Evolution with MUC

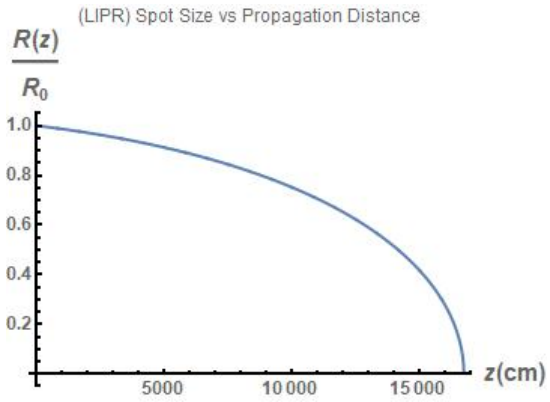

Figure 3.4: Spot size evolution in LIPR

As expected, spot size in Figure 2.1 and 3.4 evolve in a similar fashion. The main difference is the focusing point in the propagation direction. As explained in split-step Fourier method, this phenomenon occurs because of the number density addition to the differential equations. Furthermore, one should note that initial parameters used in Figure 2.1 and Figure 3.4 are the same. Therefore, only variable that could be resulting a change in focusing distance is the addition of plasma, ionization and bound electron terms to the propagation equation of the short pulse laser.

Examining the spot size brings clues about the evolution of the intensity as well since intensity and spot size are directly related to each other. It also clearly shows the focusing that arises from the non-linear terms, i.e, Kerr effect. While Kerr effect is dominant on the evolution of the pulse, self-focusing could be observed until ionization effects take place. Since ionization effects are negligible in the low intensity propagation regime, dominant nonlinear effect that is applied on the short pulse laser is Kerr effect. In order to inspect the evolution of spot size in the high intensity propagation regime, one must extrapolate the results gathered from the system of differential equations that used in the method of undetermined coefficients. However, extrapolation results for spot size are not in this interest of this study since post-ionization regime is not in the scope of this work. Furthermore, without using extrapolation, one could solve the total propagation equation that includes Raman effect and relativistic effect in order to estimate the post-ionization region.

3.2.2 Simulations for Pulse Length Evolution with MUC

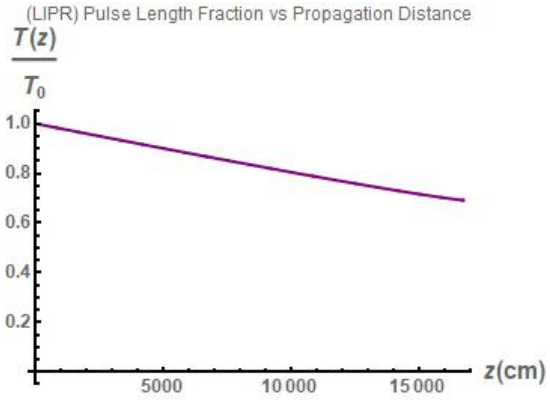

Figure 3.5: Pulse length evolution in LIPR

Figure 3.5 indicates the similar behavior as mentioned above. However, the value of the pulse length at where pulse became focused in the solution for non-ionizing problem is less than the pulse length solution with ionization problem. Approximate values could be given as ≈ 0.4 of the initial pulse length in the non-ionizing solution, ≈ 0.6 in the ionizing solution. This difference occurs because of the ionization terms in the solution affects both pulse length, and power as well. Graphically, ionization effects reduces the slope of pulse length. Same effect has to be applicable for power as well in order to conserve total energy in the low intensity propagation regime. Furthermore, pulse length is one of the most important quantities to check for whether the pulse is getting intense or not. Since pulse length is related with the frequency of the short pulse laser, and direct dependency of frequency and energy of the pulse would give whether the pulse is sufficiently intense to ionize the medium or not. However, this indirect relation with pulse length and intensity may not be clear enough to see whether the pulse getting intense. For high intensity propagation regime, this behavior should explain the focusing phenomenon well enough. However, in order to indicate the behavior of pulse length in the high intensity propagation regime, one must either solve the propagation equation with Raman and relativity terms since intensity is high enough, one cannot neglect those source terms or extrapolate the results for pulse length.

3.2.3 Simulations for Intensity Evolution with MUC

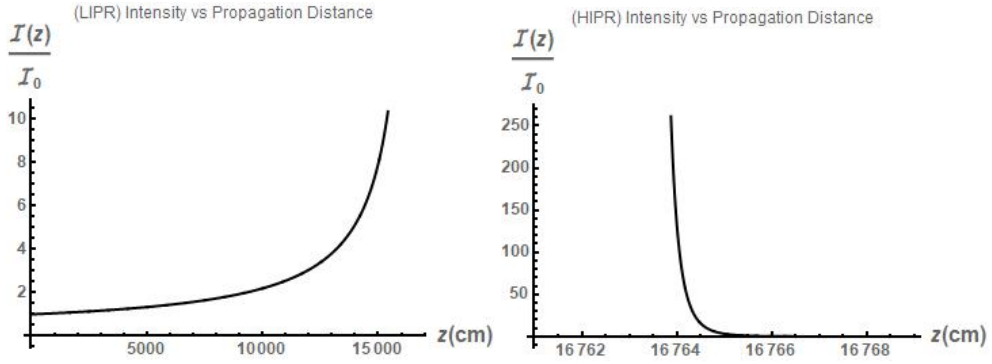

Figure 3.6: Intensity evolution in LIPR and HIPR

As stated for the spot size, intensity could be expressed as a function of power and spot size, i.e, $I = 2P/\pi R^2$. Therefore, smaller spot size and larger power would yield a larger intensity as propagation distance increases. Figure 3.6 proves that intensity increase occurs in the low intensity propagation regime. Near ionization, intensity reaches to a point where $I(z) \approx 300I_0$. It is an excellent indicator for the boundaries of high intensity propagation regime.

One could state that behavior of the field amplitude introduced in split step Fourier method and the intensity behavior introduced in Figure 3.6 are in a similar fashion since field amplitude of the short pulse laser is directly related to the intensity of the pulse. Therefore, using the Figure 3.6, validity of the solution using split step Fourier method could be possible although the values of field amplitude and the intensity of the short pulse laser is different.

Furthermore, in high intensity propagation regime, since ionization effects takes place, energy carried by pulse should decrease, that result in a decrease in intensity. This behavior could be seen in Figure 3.6 clearly. One could expect similar behavior for power of the pulse and energy of the pulse since intensity decrease only explained by energy loss in the pulse. However, before simulating these results, one could expect such behavior since energy depletion source term is explicitly added to the propagation equation of the short pulse laser.

3.2.4 Simulations for Number Density Evolution with MUC

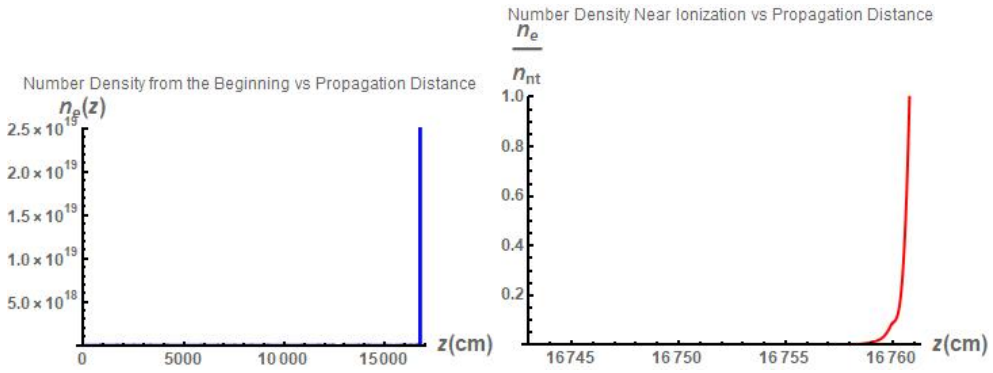

(a) Number density vs. propagation distance (b) Number density vs. propagation distance

Figure 3.7: Number density evolution with near ionization and full propagation range

While intensity reaches to a critical point that is sufficient to ionize the medium, number density becomes dominant in the propagation equation. Therefore, it would increase to a point where there are no neutral atoms to be ionized for this specific case. Figure 3.7 indicates that neutrals in the medium have been fully ionized at the end of the high intensity propagation regime. One could state the difference in number density between split-step Fourier method model and method of undetermined coefficients that medium is fully ionized in method of undetermined coefficients. As explained in split-step Fourier method, full ionization was expected near $\approx 167m$ to $\approx 170m$. Step size in split-step Fourier method was not sufficient to indicate such resolution. However, in method of undetermined coefficients, that resolution could be achieved. Keeping in mind that this model is to examine both low intensity propagation regime and high intensity propagation regime. Therefore, evolution in post-ionization region will not be discussed.

Furthermore, one should keep in mind that electron number density is not permanent and should be supplied energy by a source which is the pulse in that case. For one pulse only, this number density must be considered temporary since one pulse only focus at that point and temporarily ionize the region. In order to have a consistent number density at the focal point of the short pulse laser, continuous and consecutive pulses should be sent since $\partial n_e/\partial \tau \approx |\epsilon|^2$.

3.2.5 Simulations for Power Evolution with MUC

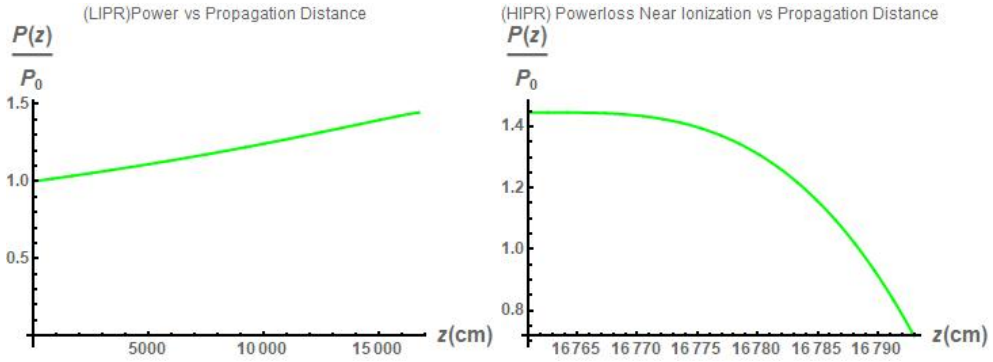

(a) Power vs. propagation distance in LIPR (b) Power vs. propagation distance in HIPR

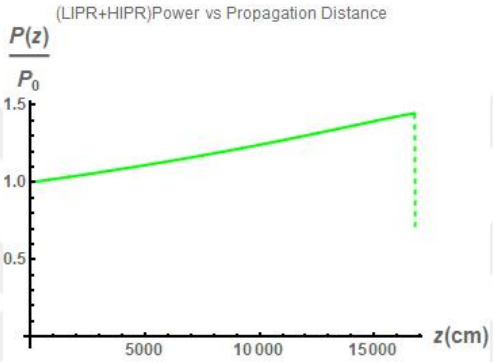

(c) Power vs. propagation distance in LIPR and HIPR (Dashed:HIPR)

Figure 3.8: Power Evolution of the pulse in LIPR and HIPR

Power evolution is one of the most important parameters to check whether the solution for propagation with ionization holds true or not. It is because powerloss has expected because of the ionization processes occurring in the medium. One could indicate the powerloss in the Figure 3.8 that solution for the propagation with ionization is sensible.

After the pulse travel a specified distance in the medium in the low intensity propagation regime, ionization terms become dominant in the propagation equation and since the derivative of the power of the pulse consists a negative number density term, focusing effects become negligible as number density increases in the medium. Hence, this phenomenon results in a powerloss as pulse propagates through the medium.

3.2.6 Simulations for Energy Evolution with MUC

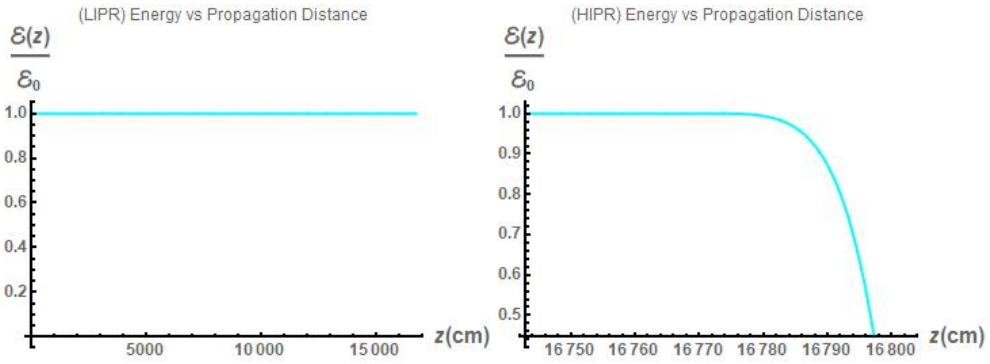

(a) Energy vs. propagation distance in LIPR (b) Energy vs. propagation distance in HIPR

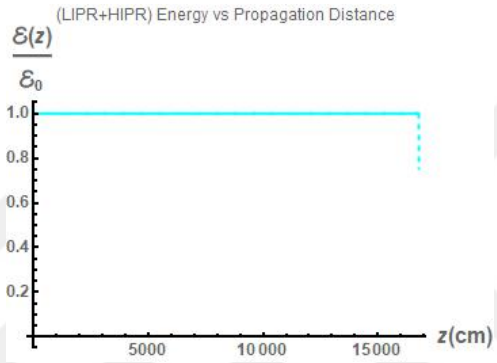

(c) Energy vs. propagation distance in LIPR and HIPR (Dashed:HIPR)

Figure 3.9: Energy Evolution of the pulse in LIPR and HIPR

One could expect a similar loss occurred in the power would repeat in the energy as well. Physically, as pulse ionizes the medium, there has to be an energy depletion since the total energy of the system has to be conserved. As Figure 3.9 indicates the evolution of the energy, expectation and model behavior matches.

As expected, in the low intensity propagation regime energy is conserved. There is a very small change in energy that could not be seen because of extremely small ionization in the medium but this change assumed to be negligible. However, when medium starts to ionize, this energy has to be supplied by the pulse itself. Hence, it yields a loss in energy for the pulse.

CHAPTER 4

CONCLUSION

A semi-analytical way to solve the propagation equation for the propagation equation of a short pulse laser in a non-linear optical medium brings to be able to examine the evolution in terms of the wave parameters, such as spot size, pulse length, intensity, and power. Those parameters clearly show the behavior of the short-pulse laser in the high intensity propagation regime. Since one can expect an energy loss for the pulse in the high intensity propagation regime without explicitly solving the propagation equation by only checking the dissipation terms, those expectations could be clearly seen from the simulations by solving the propagation equation with the method of undetermined coefficients, unlike the split-step Fourier method. However, if only the electron number density is concerned, both methods yield viable results if the parameters of the split-step Fourier method has tuned well. Therefore, in order to fully examine the behavior of the pulse, a semi-analytical solution might give more clear results than a numerical method.

The split-step Fourier method is one of the most sophisticated approaches for solving non-linear Schrödinger type equations. Although using methods such as source dependant expansion or variational analysis for solving a propagation equation for a Gaussian pulse including ionization terms could yield more accurate results analytically, the split-step Fourier method would be beneficial for ease of utilization and acceptable range of error. Alongside solving this propagation equation with the split-step Fourier method, using one external method, such as the method of undetermined coefficients, would be helpful to check whether the numerical method utilized for solving the system could be assumed to be valid or not. By validating that two solutions that have been gathered from the split-step Fourier method and method of

undetermined coefficients match, one could state that these methods should agree on the previous solutions from the literature in the low intensity propagation regime. Since it has been shown that evolutions of the propagation equation by utilizing both split-step Fourier method and method of undetermined coefficients are compatible in the low intensity propagation regime, it could be concluded that solving the propagation equation with included ionization effects with split-step Fourier method and method of undetermined coefficients yield a reliable solution.

The differential equation that arises from the general propagation equation could already give a clue about how the evolution of the Gaussian pulse could occur in the high intensity propagation regime. One could examine the all differential equation and state that there needs to be an explicit power and energy loss if the intensity of the Gaussian pulse is sufficient enough to partially ionize the region. This expectation has met by explicitly solving the system of differential equations of the pulse propagation. As in both literature solutions for low intensity propagation regime and neglecting very small terms of ionization terms in the propagation equation, power and energy should be conserved in the low intensity propagation regime. However, when ionization terms become significant and could not be negligible, ionization terms would dominate the propagation. Since the total energy of the system has to be conserved, ionization energy needs to be supplied by the electromagnetic pulse itself. Therefore it has to yield a power and energy loss in the high intensity propagation regime. Furthermore, power and energy loss is not in a linear trend, contrarily, it has an exponential decrease pattern. This exponential decrease brings an electron number density evolution that has a very small increase in the low intensity propagation regime but a significant increase in the high intensity propagation regime. This behavior could be also shown from the split step Fourier method solution of field amplitude. Field amplitude slowly increases in the low intensity propagation regime but this change could not easily detectable if one compares this with the change in the high intensity propagation regime. Field amplitude reaches a point where the medium starts to ionize and eventually brings a fully ionized medium. However, one could state that results from the split-step Fourier method only yield field amplitude and number density. Although it is possible to gather all the pulse parameters that are, spot size, pulse length, intensity, and power, all those different equations for these parameters need

to be applied with the split-step Fourier method. After obtaining all the equations for wave parameters, it is pointless to utilize the split-step Fourier method for these equations separately since this method is beneficial for solving the propagation equation without explicitly examining the wave parameters. Furthermore, spot size and pulse length evolution are expected to behave similarly with the solution for non-ionizing solutions for Gaussian pulse in literature with a difference of focal point for spot size and difference in the value at the end of the propagation for pulse length. Since the differential equation for spot size clearly indicates there is an electron number density contribution, it is expected to focus at a shorter distance. Also, pulse length evolution is directly related to the spot size evolution and yield less steepness in the evolution for pulse length since the focal point is much shorter and behavior of the pulse length is similar yielding longer pulse length at the end of the pulse if one compares this with the solution with non-ionizing problem.

It is shown that using the split-step Fourier method and method of undetermined coefficients met the expectations from examining the propagation equation well. Furthermore, solutions gathered from these two methods are behaving harmoniously and validating each other. Hence, one could conclude that although there are some different error-prone while using the split-step Fourier method related to step size selection trade-offs and error in the method of undetermined coefficients related to Taylor expansion, it is convenient to use those methods while struggling with a non-linear Schrödinger equation type problem.

APPENDICES

A. Source Code for Split-Step Fourier Method in Python

```
import numpy as np
from plotly.offline import plot
import plotly.graph_objs as go
from math import factorial
import scipy.fftpack


def s_n(number):
    a, b = '{:.4E}'.format(number).split('E')
    return '{:.5f}E{:+03d}'.format(float(a)/10,
     ↪  int(b)+1)


np.seterr(all="warn")
# Initials
lambda_zero = 0.775 * 10**(-4)
k_zero = 2 * np.pi / lambda_zero
c = 3 * 10**10
n_zero = 1
n_two = 3 * 10**(-19)
omega_zero = (c * k_zero) / n_zero
R_zero = 1
T_zero = 0.66 * 10**(-12)
P_NL = (lambda_zero**2) / (2 * np.pi * n_zero * n_two)
P_zero = P_NL
alpha_zero = 0.5
beta_zero = -20
beta_two = 2.2 * 10**(-31)
U_ion = 14.35
Kappa = 8
I_mp = 5.6e13
```

```
q = 1.6 * 10**(-19)
m = 9.31 * 10**(-31)
n_atm = 2.5e19
sigma_k = 2.88 * 10**(-99 / 8)
epsilon_zero = 8.84e-12
pi = 3.1415926535

ln = 0
alpha = 0
alph = alpha/4.343
gamma = (((omega_zero**2) * (n_zero**2) * n_two) / (4 *
 ↪  np.pi * c))
to = T_zero
ro = R_zero
Ld = (to**2)/np.absolute(beta_two)/33
tau = np.arange(-0.8e-12, 0.8e-12, 0.008e-12)
r = np.linspace(-5.001, 5.001, 200)
Po = (16 * P_zero) / (c * n_zero * R_zero**2)
Ao = np.sqrt(Po)
dt = 0.003e-12
dr = 0.025
rel_error = 1e-5
z_max = 1.11
z_min = 0.1
h = 1500

op_pulse = [[0 for y in tau] for x in np.arange(z_min,
 ↪  z_max, z_min)]
pbratio = [0 for x in np.arange(z_min, z_max, z_min)]
phadisp = [0 for x in np.arange(z_min, z_max, z_min)]
number_density = [0 for x in np.arange(z_min, z_max,
 ↪  z_min)]

uaux = Ao * np.exp(-(1+1j*(-beta_zero))*(tau/to)**2 -
 ↪  (1+1j*(-alpha_zero))*(r/ro)**2)
uamp = Ao

for ii in np.arange(z_min, z_max, z_min):
    z = ii
    print(Ld)
    u = uaux[:]
```

```
68      n = number_density[:]
69      l = np.max(u.shape)
70      fwhml = np.nonzero(np.absolute(u) >
        ↪  np.absolute(np.max(np.real(u))/2.0))
71      fwhml = len(fwhml[0])
72
73      dw_t = 1.0 / float(l) / dt * 2.0 * pi
74      dw_r = 1.0 / float(l) / dr * 2.0 * pi
75
76      w_t = dw_t*np.arange(-1 * l / 2.0, l / 2.0, 1)
77      w_t = np.asarray(w_t)
78      w_t = np.fft.fftshift(w_t)
79      w_r = dw_r * np.arange(-1 * l / 2.0, l / 2.0, 1)
80      w_r = np.asarray(w_r)
81      w_r = np.fft.fftshift(w_r)
82
83      u = np.asarray(u)
84      u = np.fft.fftshift(u)
85      spectrum = np.fft.fft(np.fft.fftshift(u))
86      spectrum = np.array(spectrum, dtype=np.complex128)
87
88      for jj in np.arange(h, z*Ld, h):
89          spectrum = spectrum * np.exp((1 / (2.0 * 1j *
            ↪  k_zero)) *
90                                       (-(h / 2.0) *
                                         ↪  np.power(w_r,
                                         ↪  2) + k_zero *
                                         ↪  beta_two *
                                         ↪  np.power(w_t,
                                         ↪  2) * (h /
                                         ↪  2.0)))
91
92          f = np.fft.ifft(spectrum)
93          intensity = np.array(np.absolute((np.absolute(f)
            ↪  * (Po * c * n_zero / 8 * pi)) / uaux[99]))
94          density_deriv = np.array(2 * pi * omega_zero /
            ↪  factorial(Kappa) * (intensity / I_mp)**Kappa
            ↪  * n_atm)
95          omega_plasma_square = np.array(((4 * pi * q**2
            ↪  * np.trapz(density_deriv)) / m) / c ** 2))
96          f = f * (1 + ((1 / (2.0 * 1j * k_zero) *
```

```
97                              (- gamma *
                                 ↪  np.power(np.absolute(f), 2)
                                 ↪  * h + h *
                                 ↪  omega_plasma_square / c ** 2
                                 ↪  -
98                              (h * 1j * (8.0 * pi * k_zero) /
                                ↪  c) * (U_ion /
                                ↪  np.power(np.absolute(f), 2))
99                               * (2 * pi * n_atm *
                                  ↪  density_deriv * omega_zero
                                  ↪  / factorial(Kappa)) *
100                               (((2 * P_zero)/(pi *
                                  ↪  R_zero**2))/I_mp)**Kappa))))
101         f = np.array(f, dtype=np.complex128)
102
103         spectrum = np.fft.fft(f)
104         spectrum = spectrum * np.exp((1 / (2 * 1j *
             ↪  k_zero)) *
105                                      (-(h / 2) *
                                         ↪  np.power(w_r,
                                         ↪  2) + k_zero *
                                         ↪  beta_two *
                                         ↪  np.power(w_t,
                                         ↪  2) * (h / 2)))
106
107     f = np.fft.ifft(spectrum)
108     I_rzt = np.absolute((np.absolute(f) * (Po * c *
         ↪  n_zero / 8 * pi)) / uaux[99])
109     number_density_function = np.trapz(2 * pi *
         ↪  omega_zero / factorial(Kappa) * (I_rzt /
         ↪  I_mp)**Kappa * n_atm, dx=z*Ld)
110     number_density[ln] = number_density_function
111     op_pulse[ln] = np.absolute(f)
112     print(s_n(I_rzt[99]))
113     fwhm = np.nonzero(np.absolute(f) >
         ↪  np.absolute(np.max(np.real(f))/2.0))
114     fwhm = len(fwhm[0])
115     ratio = float(fwhm)/fwhml
116     pbratio[ln] = ratio
117     im = np.absolute(np.imag(f))
118     re = np.absolute(np.real(f))
```

```
119         div = np.dot(im, np.linalg.pinv([re]))
120         dd = np.degrees(np.arctan(div))
121         phadisp[ln] = dd[0]
122         print("Progress: " + "> %d / " % ln +
            ↪  str(len(op_pulse)))
123         ln = ln + 1
124
125     # Plots
126     print("\n\n> Plotting...")
127     trace_pulse_evolution = go.Surface(z=op_pulse,
            ↪  colorscale='Jet', y=np.arange(h, h * (ln + 1), h),
128                                        x=np.linspace(r[0],
                                           ↪  r[-1], 200))
129     # trace_pulse_evolution = go.Scatter3d(z=np.arange(h, h
            ↪  * (ln + 1), h), y=tau,
130     #                                      x=r,
            ↪  marker=dict(size=12, color=op_pulse,
            ↪  colorscale='Jet', opacity=0.8))
131     trace_pulse_broad = go.Scatter(y=pbratio[0:ln],
            ↪  x=np.arange(1, ln+1, 1))
132     trace_phase_change = go.Scatter(y=phadisp[0:ln],
            ↪  x=np.arange(1, ln+1, 1))
133     # trace_number_density = go.Surface(z=number_density,
            ↪  colorscale='Jet', y=np.arange(h, h * (ln + 1), h))
134     trace_number_density =
            ↪  go.Scatter(y=number_density[0:ln], x=np.arange(h, h
            ↪  * (ln + 1), h))
135     trace_input_pulse = go.Scatter(y=np.absolute(uaux))
136     layout_input_pulse = go.Layout(
137         autosize=False,
138         width=500,
139         height=400,
140         title='Input Pulse',
141         xaxis=dict(
142             title='Time',
143             titlefont=dict(
144                 family='Courier New, monospace',
145                 size=18,
146                 color='#7f7f7f'
147             )
148         ),
```

```
149         yaxis=dict(
150             title='Amplitude',
151             titlefont=dict(
152                 family='Courier New, monospace',
153                 size=18,
154                 color='#7f7f7f'
155             )
156         )
157     )
158     layout_number_2d = go.Layout(
159         autosize=False,
160         width=500,
161         height=400,
162         title='Number Density',
163         xaxis=dict(
164             title='z(cm)',
165             titlefont=dict(
166                 family='Courier New, monospace',
167                 size=18,
168                 color='#7f7f7f'
169             )
170         ),
171         yaxis=dict(
172             title='Number Density',
173             titlefont=dict(
174                 family='Courier New, monospace',
175                 size=18,
176                 color='#7f7f7f'
177             )
178         )
179     )
180
181     layout_pulse_evolution = go.Layout(
182         autosize=False,
183         width=800,
184         height=800,
185         title='Pulse Evolution',
186         scene=go.Scene(
187             xaxis=go.XAxis(title='r(cm)'),
188             yaxis=go.YAxis(title='z(cm)'),
189             zaxis=go.ZAxis(title='Field Amplitude'))
```

```
)

layout_number_density = go.Layout(
    autosize=False,
    width=800,
    height=800,
    title='Number Density',
    scene=go.Scene(
        xaxis=go.XAxis(title='Time&Radius'),
        yaxis=go.YAxis(title='z(cm)'),
        zaxis=go.ZAxis(title='Number Density'))

)
layout_pulse_contour = go.Layout(
    autosize=False,
    width=600,
    height=400,
    title='Pulse Evolution Near Ionization',
    xaxis=dict(
        title='r(cm)',
        titlefont=dict(
            family='Courier New, monospace',
            size=18,
            color='#7f7f7f'
        )
    ),
    yaxis=dict(
        title='z(cm)',
        titlefont=dict(
            family='Courier New, monospace',
            size=18,
            color='#7f7f7f'
        )
    )
)
print(np.shape(op_pulse))
test_pulse = op_pulse[9:]
print(np.shape(test_pulse))
pulse_evolution_contour =
 ↪  go.Figure(data=go.Contour(z=test_pulse, x=r,
 ↪  y=np.arange(10*h, 12*h, h),colorbar=dict(nticks=10,
```

```
229 title="Amplitude", ticks='outside',ticklen=5,
    ↪ tickwidth=1,showticklabels=True,tickangle=0,
230 tickfont_size=12)),layout=layout_pulse_contour)
231 pulse_evolution =
    ↪ go.Figure(data=[trace_pulse_evolution],
    ↪ layout=layout_pulse_evolution)
232
233 input_pulse = go.Figure(data=[trace_input_pulse],
    ↪ layout=layout_input_pulse)
234
235 number_evolution =
    ↪ go.Figure(data=[trace_number_density],
    ↪ layout=layout_number_2d)
236
237 plot([trace_phase_change],
    ↪ filename='./phase_change.html')
238 plot([trace_pulse_broad],
    ↪ filename='./pulse_broadening.html')
239 plot(pulse_evolution, filename='./pulse_evolution.html')
240 plot(input_pulse, filename='./input_pulse.html')
241 plot(number_evolution,
    ↪ filename='./number_density.html',)
242 plot(pulse_evolution_contour,
    ↪ filename='./pulse_evolution_contour.html')
```

B. Source Code for Method of Undetermined Coefficients for Differential Equations in Mathematica

```
In[•]:= A[r, z, τ] := Sqrt[16 P[z] / (c n0 (R[z])^2)] Exp[I θ[z] - (1 + I α[z]) r^2 / (R[z])^2 - (1 + I β[z]) τ^2 / (T[z])^2]

Δ[r, z, τ] := Sqrt[16 P[z] / (c n0 (R[z])^2)] Exp[-I θ[z] - (1 - I α[z]) r^2 / (R[z])^2 - (1 - I β[z]) τ^2 / (T[z])^2]

S[r, z, τ] := A[r, z, τ] (Sqrt[16 P[z] / (c n0 (R[z])^2)] Exp[- I θ[z] - (1 - I α[z]) r^2 / (R[z])^2 - (1 - I β[z]) τ^2 / (T[z])^2])

In[•]:= Ne := ne[z] Exp[-2 κ r^2 / R[z]^2] Exp[-2 κ τ^2 / T[z]^2]

ωp := Sqrt[4 Pi q^2 Ne / m]

In[•]:= eqn := 1/r D[r D[A[r, z, τ], r], r] + 2 I k0 D[A[r, z, τ], z] - k0 β2 D[D[A[r, z, τ], τ], τ] +
c n0 / (2 PNL) S[r, z, τ] × A[r, z, τ] + (ωp)^2 / (ω0)^2 c^2 S[r, z, τ] × A[r, z, τ] - I λMPI / S[r, z, τ] (2 P[z] / (Pi R[z]^2))^κ A[r, z, τ]

Expand[FullSimplify[eqn Δ[r, z, τ] / S[r, z, τ]]]

Out[•]= 4 r^2 / R[z]^4 - 4 / R[z]^2 + 8 e^(-2 r^2/R[z]^2 - 2 τ^2/T[z]^2) P[z] / (R[z]^2 PNL) - i 2^(-4+κ) c e^(2 r^2/R[z]^2 + 2 τ^2/T[z]^2) π^(-κ) (P[z] / R[z]^2)^(-1+κ) n0 λMPI - 4 τ^2 k0 β2 / T[z]^4 +
2 k0 β2 / T[z]^2 + 8 i r^2 α[z] / R[z]^4 - 4 i α[z] / R[z]^2 - 4 r^2 α[z]^2 / R[z]^4 - 8 i τ^2 k0 β2 β[z] / T[z]^4 + 2 i k0 β2 β[z] / T[z]^2 + 4 τ^2 k0 β2 β[z]^2 / T[z]^4 +
64 e^(-2 (1+κ) (r^2/R[z]^2 + τ^2/T[z]^2)) π q^2 P[z] ne[z] / (c^3 m R[z]^2 n0 ω0^2) + i k0 P'[z] / P[z] + 4 i r^2 k0 R'[z] / R[z]^3 - 2 i k0 R'[z] / R[z] -
4 r^2 k0 α[z] R'[z] / R[z]^3 + 4 i τ^2 k0 T'[z] / T[z]^3 - 4 τ^2 k0 β[z] T'[z] / T[z]^3 + 2 r^2 k0 α'[z] / R[z]^2 + 2 τ^2 k0 β'[z] / T[z]^2 - 2 k0 θ'[z]
```

In[•]:=
$$\text{RealPart} := \frac{4r^2}{R[z]^4} - \frac{4}{R[z]^2} + \frac{8e^{-\frac{2r^2}{R[z]^2}-\frac{2\tau^2}{T[z]^2}}P[z]}{R[z]^2 P_{NL}} - \frac{4\tau^2 k_0 \beta_2}{T[z]^4} + \frac{2k_0\beta_2}{T[z]^2} - \frac{4r^2\alpha[z]^2}{R[z]^4} + \frac{4\tau^2 k_0 \beta_2 \beta[z]^2}{T[z]^4} +$$
$$\frac{64e^{-2(1+\kappa)\left(\frac{r^2}{R[z]^2}+\frac{\tau^2}{T[z]^2}\right)}\pi q^2 P[z] n_e[z]}{c^3 m R[z]^2 n_0 \omega_0^2} - \frac{4r^2 k_0 \alpha[z] R'[z]}{R[z]^3} - \frac{4\tau^2 k_0 \beta[z] T'[z]}{T[z]^3} + \frac{2r^2 k_0 \alpha'[z]}{R[z]^2} +$$
$$\frac{2\tau^2 k_0 \beta'[z]}{T[z]^2} - 2k_0\theta'[z]$$

$$\text{ImaginaryPart} := -2^{-4+\kappa} c e^{\frac{2r^2}{R[z]^2}+\frac{2\tau^2}{T[z]^2}} \pi^{-\kappa}\left(\frac{P[z]}{R[z]^2}\right)^{-1+\kappa} n_0 \lambda_{MPI} + \frac{8r^2\alpha[z]}{R[z]^4} - \frac{4\alpha[z]}{R[z]^2} -$$
$$\frac{8\tau^2 k_0 \beta_2 \beta[z]}{T[z]^4} + \frac{2k_0\beta_2\beta[z]}{T[z]^2} + \frac{k_0 P'[z]}{P[z]} + \frac{4r^2 k_0 R'[z]}{R[z]^3} - \frac{2k_0 R'[z]}{R[z]} + \frac{4\tau^2 k_0 T'[z]}{T[z]^3}$$

In[•]:=
$$\text{RealPartExpandedOnce} := \text{RealPart} /. e^{-\frac{2r^2}{R[z]^2}-\frac{2\tau^2}{T[z]^2}} \to \left(1 - \frac{2r^2}{R[z]^2} - \frac{2\tau^2}{T[z]^2}\right)$$

$$\text{RealPartExpandedTwice} := \text{RealPartExpanded} /. e^{-2(1+\kappa)\left(\frac{r^2}{R[z]^2}+\frac{\tau^2}{T[z]^2}\right)} \to \left(1 - 2(1+\kappa)\left(\frac{r^2}{R[z]^2}+\frac{\tau^2}{T[z]^2}\right)\right)$$

In[•]:=
$$\text{ImaginaryPartExpanded} := \text{ImaginaryPart} /. e^{\frac{2r^2}{R[z]^2}+\frac{2\tau^2}{T[z]^2}} \to \left(1 + \frac{2r^2}{R[z]^2} + \frac{2\tau^2}{T[z]^2}\right)$$

In[•]:=
$$\text{Expand}[\text{RealPartExpandedTwice}]$$

Out[•]=
$$\frac{4r^2}{R[z]^4} - \frac{4}{R[z]^2} - \frac{16r^2 P[z]}{R[z]^4 P_{NL}} + \frac{8P[z]}{R[z]^2 P_{NL}} - \frac{4\tau^2 k_0 \beta_2}{T[z]^4} - \frac{16\tau^2 P[z]}{R[z]^2 P_{NL} T[z]^2} + \frac{2k_0\beta_2}{T[z]^2} -$$
$$\frac{4r^2\alpha[z]^2}{R[z]^4} + \frac{4\tau^2 k_0 \beta_2 \beta[z]^2}{T[z]^4} - \frac{128\pi q^2 r^2 P[z] n_e[z]}{c^3 m R[z]^4 n_0 \omega_0^2} - \frac{128\pi q^2 r^2 \kappa P[z] n_e[z]}{c^3 m R[z]^4 n_0 \omega_0^2} +$$
$$\frac{64\pi q^2 P[z] n_e[z]}{c^3 m R[z]^2 n_0 \omega_0^2} - \frac{128\pi q^2 \tau^2 P[z] n_e[z]}{c^3 m R[z]^2 n_0 \omega_0^2 T[z]^2} - \frac{128\pi q^2 \kappa \tau^2 P[z] n_e[z]}{c^3 m R[z]^2 n_0 \omega_0^2 T[z]^2} -$$
$$\frac{4r^2 k_0 \alpha[z] R'[z]}{R[z]^3} - \frac{4\tau^2 k_0 \beta[z] T'[z]}{T[z]^3} + \frac{2r^2 k_0 \alpha'[z]}{R[z]^2} + \frac{2\tau^2 k_0 \beta'[z]}{T[z]^2} - 2k_0\theta'[z]$$

In[•]:= `Thread[CoefficientList[RealPartExpandedTwice, {r, τ}] == 0]`

Out[•]=
$$\left\{\left\{-\frac{4}{R[z]^2}+\frac{8P[z]}{R[z]^2 P_{NL}}+\frac{2k_0\beta_2}{T[z]^2}+\frac{64\pi q^2 P[z] n_e[z]}{c^3 m R[z]^2 n_0 \omega_0^2}-2k_0\theta'[z],\ 0,\ -\frac{4k_0\beta_2}{T[z]^4}-\frac{16P[z]}{R[z]^2 P_{NL} T[z]^2}+\right.\right.$$
$$\left.\frac{4k_0\beta_2\beta[z]^2}{T[z]^4}-\frac{128\pi q^2(1+\kappa)P[z]n_e[z]}{c^3 m R[z]^2 n_0\omega_0^2 T[z]^2}-\frac{4k_0\beta[z]T'[z]}{T[z]^3}+\frac{2k_0\beta'[z]}{T[z]^2}\right\}==0,\ \{0,0,0\}==0,$$
$$\left.\left\{\frac{4}{R[z]^4}-\frac{16P[z]}{R[z]^4 P_{NL}}-\frac{4\alpha[z]^2}{R[z]^4}-\frac{128\pi q^2(1+\kappa)P[z]n_e[z]}{c^3 m R[z]^4 n_0\omega_0^2}-\frac{4k_0\alpha[z]R'[z]}{R[z]^3}+\frac{2k_0\alpha'[z]}{R[z]^2},0,0\right\}==0\right\}$$

In[•]:= `Thread[CoefficientList[ImaginaryPartExpanded, {r, τ}] == 0]`

Out[•]=
$$\left\{\left\{-2^{-4+\kappa}c\pi^{-\kappa}\left(\frac{P[z]}{R[z]^2}\right)^{-1+\kappa}n_0\lambda_{MPI}-\frac{4\alpha[z]}{R[z]^2}+\frac{2k_0\beta_2\beta[z]}{T[z]^2}+\frac{k_0P'[z]}{P[z]}-\frac{2k_0R'[z]}{R[z]},\right.\right.$$
$$\left.0,\ -\frac{2^{-3+\kappa}c\pi^{-\kappa}\left(\frac{P[z]}{R[z]^2}\right)^{-1+\kappa}n_0\lambda_{MPI}}{T[z]^2}-\frac{8k_0\beta_2\beta[z]}{T[z]^4}+\frac{4k_0T'[z]}{T[z]^3}\right\}==0,$$
$$\{0,0,0\}==0,\left\{-\frac{2^{-3+\kappa}c\pi^{-\kappa}\left(\frac{P[z]}{R[z]^2}\right)^{-1+\kappa}n_0\lambda_{MPI}}{R[z]^2}+\frac{8\alpha[z]}{R[z]^4}+\frac{4k_0R'[z]}{R[z]^3},0,0\right\}==0\Bigg\}$$

C. Source Code for Method of Undetermined Coefficients for Differential Equations in Mathematica

```
In[•]:= λ0 := 0.775 × 10^(-4)
        k0 := 2 π / λ0
        c := 3 × 10^(10)
        n0 := 1
        n2 := 3 × 10^(-19)
        ω0 := c k0 / n0
        ℛ0 := 1
        𝒯0 := 0.66 × 10^(-12)
        𝒫NL := (λ0)^2 / (2 π n0 n2)
        𝒫0 := 𝒫NL
        α0 := 0.5
        β0 := -20
        β2 := 2.2 × 10^(-31)
        Uion := 14.35
        κ := 8
        re := 2.8 × 10^-13
        nn := 0.02504 × 10^21
        Imp := 5.8 × 10^13
        Z := 16763
        q := 1.6 × 10^-19
        m := 9.1 × 10^-31
        λMPI := (8 π k0 / c) (Uion / Imp^κ)

In[•]:= eqn1 := -4/R[z]^2 + 8 P[z]/(R[z]^2 𝒫NL) + 2 k0 β2/T[z]^2 + 64 π q^2 P[z] ne[z]/(c^3 m R[z]^2 n0 ω0^2) - 2 k0 θ'[z]

        eqn2 := -4 k0 β2/T[z]^4 - 16 P[z]/(R[z]^2 𝒫NL T[z]^2) + 4 k0 β2 β[z]^2/T[z]^4 - 128 π q^2 (1 + κ) P[z] ne[z]/(c^3 m R[z]^2 n0 ω0^2 T[z]^2) - 4 k0 β[z] T'[z]/T[z]^3 + 2 k0 β'[z]/T[z]^2

        eqn3 := 4/R[z]^4 - 16 P[z]/(R[z]^4 𝒫NL) - 4 α[z]^2/R[z]^4 - 128 π q^2 (1 + κ) P[z] ne[z]/(c^3 m R[z]^4 n0 ω0^2) - 4 k0 α[z] R'[z]/R[z]^3 + 2 k0 α'[z]/R[z]^2

        eqn4 := -2^(-4+κ) c π^-κ (P[z]/R[z]^2)^(-1+κ) n0 λMPI - 4 α[z]/R[z]^2 + 2 k0 β2 β[z]/T[z]^2 + k0 P'[z]/P[z] - 2 k0 R'[z]/R[z]

        eqn5 := -(2^(-3+κ) c π^-κ (P[z]/R[z]^2)^(-1+κ) n0 λMPI)/T[z]^2 - 8 k0 β2 β[z]/T[z]^4 + 4 k0 T'[z]/T[z]^3

        eqn6 := -(2^(-3+κ) c π^-κ (P[z]/R[z]^2)^(-1+κ) n0 λMPI)/R[z]^2 + 8 α[z]/R[z]^4 + 4 k0 R'[z]/R[z]^3

        eqn7 := 4 e^(-2 κ τ^2/T[z]^2) κ τ ne[z]/T[z]^2 == 2 π ω0/Factorial[κ - 1] (2 P[z]/(π R[z]^2)/Imp)^κ nn /. τ → T[z]
```

```
In[•]:= ic1 := R[0] == ℛ0
        ic2 := T[0] == 𝒯0
        ic3 := P[0] == 𝒫0
        ic4 := α[0] == α0
        ic5 := β[0] == β0
        ic6 := ne[0] == 0
        ic7 := θ[0] == 0

In[•]:= mol[n : _Integer | {_Integer ..}, o_ : "Pseudospectral"] :=
         {"MethodOfLines", "SpatialDiscretization" →
           {"TensorProductGrid", "MaxPoints" → n, "MinPoints" → n, "DifferenceOrder" → o}}
        mol[tf : False | True, sf_ : Automatic] :=
         {"MethodOfLines", "DifferentiateBoundaryConditions" → {tf, "ScaleFactor" → sf}}
        solution :=
         NDSolve[{eqn1 == 0, eqn2 == 0, eqn3 == 0, eqn4 == 0, eqn5 == 0, eqn6 == 0, eqn7, ic1, ic2, ic3,
           ic4, ic5, ic6, ic7}, {R, T, P, ne}, {z, 0, Z}, WorkingPrecision → 64, AccuracyGoal → 20,
          PrecisionGoal → 20, Method → Automatic]
        "Union[mol[1500,2],mol[True,1]]"
        solution
```

REFERENCES

[1] G. Agrawal. *Nonlinear fiber optics*, volume 160. 1990.

[2] N. Aközbek, C. M. Bowden, A. Talebpour, and S. L. Chin. özbek, N., Bowden, C. M., Talebpour, A., & Chin, S. L. (2000). Femtosecond pulse propagation in air: Variational analysis. Physical Review E - Statistical Physics, Plasmas, Fluids, and Related Interdisciplinary Topics, 61(4), 4540–4549. ht. *Physical Review E - Statistical Physics, Plasmas, Fluids, and Related Interdisciplinary Topics*, 61(4):4540–4549, apr 2000.

[3] D. Anderson and M. Bonnedal. Variational approach to nonlinear self-focusing of Gaussian laser beams. *Physics of Fluids*, 22(1):105–109, aug 1979.

[4] T. M. Baer and F. Schlachter. Lasers in Science and Industry: A report to OSTP on the contribution of lasers to American jobs and the American economy Honoring the 50th Anniversary of the Laser. Technical report.

[5] T. Bodurov. Annales de la Fondation Louis de Broglie. Technical report, 2005.

[6] R. W. Boyd. Nonlinear Optics - 3rd Edition.

[7] S. Chávez Cerda, S. B. Cavalcanti, and J. M. Hickmann. A variational approach of nonlinear dissipative pulse propagation. *European Physical Journal D*, 1(3):313–316, 1998.

[8] J. M. Cole, J. C. Wood, N. C. Lopes, K. Poder, R. L. Abel, S. Alatabi, J. S. Bryant, A. Jin, S. Kneip, K. Mecseki, D. R. Symes, S. P. Mangles, and Z. Najmudin. Laser-wakefield accelerators as hard x-ray sources for 3D medical imaging of human bone. *Scientific Reports*, 5, aug 2015.

[9] A. Couairon and L. Bergé. Modeling the filamentation of ultra-short pulses in ionizing media. *Physics of Plasmas*, 7(1):193–209, jan 2000.

[10] E. Esarey, P. Sprangle, J. Krall, and A. Ting. Self-focusing and guiding of short laser pulses in ionizing gases and plasmas. *IEEE Journal of Quantum Electronics*, 33(11):1879–1914, nov 1997.

[11] Z. F. Feng, W. Li, C. X. Yu, X. Liu, J. Liu, and L. B. Fu. Extended laser filamentation in air generated by femtosecond annular Gaussian beams. *Physical Review A - Atomic, Molecular, and Optical Physics*, 91(3):1–7, 2015.

[12] G. Fibich, S. Eisenmann, B. Ilan, Y. Erlich, M. Fraenkel, Z. Henis, A. L. Gaeta, and A. Zigler. Self-focusing Distance of Very High Power Laser Pulses. *Optics Express*, 13(15):5897, jul 2005.

[13] S. Fourmaux, S. Corde, K. Ta Phuoc, S. Buffechoux, S. Gnedyuk, A. Rousse, A. Krol, and J. C. Kieffer. Initial steps towards imaging tumors during their irradiation by protons with the 200TW laser at the Advanced Laser Light Source facility (ALLS). In K. W. D. Ledingham, W. P. Leemans, E. Esarey, S. M. Hooker, K. Spohr, and P. McKenna, editors, *Laser Acceleration of Electrons, Protons, and Ions; and Medical Applications of Laser-Generated Secondary Sources of Radiation and Particles*, volume 8079, page 80791I. SPIE, may 2011.

[14] M. Ganguly, S. Miller, and K. Mitra. Model development and experimental validation for analyzing initial transients of irradiation of tissues during thermal therapy using short pulse lasers. *Lasers in Surgery and Medicine*, 47(9):711–722, nov 2015.

[15] T. M. Jeong and J. Lee. Generation of High-Intensity Laser Pulses and their Applications. In *High Energy and Short Pulse Lasers*. InTech, sep 2016.

[16] S. Kawata, T. Izumiyama, T. Nagashima, M. Takano, D. Barada, Q. Kong, Y. J. Gu, P. X. Wang, Y. Y. Ma, and W. M. Wang. Laser ion acceleration toward future ion beam cancer therapy - Numerical simulation study -. *LASER THERAPY*, 22(2):103–114, 2013.

[17] J. C. Kieffer, S. Fourmaux, and A. Krol. The ultrafast high-peak power lasers in future biomedical and medical x-ray imaging. In *19th International Conference and School on Quantum Electronics: Laser Physics and Applications*, volume 10226, page 1022612. SPIE, jan 2017.

[18] H. D. Ladouceur, A. P. Baronavski, D. Lohrmann, P. W. Grounds, and P. G. Girardi. Electrical conductivity of a femtosecond laser generated plasma channel in air. *Optics Communications*, 189(1-3):107–111, mar 2001.

[19] X. Liu, D. Du, and G. Mourou. Laser ablation and micromachining with ultrashort laser pulses. *IEEE Journal of Quantum Electronics*, 33(10):1706–1716, oct 1997.

[20] National Academies of Sciences, Engineering and Medicine. *Opportunities in Intense Ultrafast Lasers: Reaching for the Brightest Light*. National Academy of Sciences, mar 2018.

[21] S. Nikumb, Q. Chen, C. Li, H. Reshef, H. Y. Zheng, H. Qiu, and D. Low. Precision glass machining, drilling and profile cutting by short pulse lasers. In *Thin Solid Films*, volume 477, pages 216–221. Elsevier, apr 2005.

[22] K. Nouri, M. L. Elsaie, V. Vejjabhinanta, M. Stevens, S. S. Patel, C. Caperton, and G. Elgart. Comparison of the effects of short- and long-pulse durations when using a 585-nm pulsed dye laser in the treatment of new surgical scars. *Lasers in Medical Science*, 25(1):121–126, jan 2010.

[23] H. Oliver, R. Deiterding, R. Glowinski, S. Poole, H. Oliver, and S. Poole. A Reliable Split-Step Fourier Method for the Propagation Equation of Ultra-Fast Pulses in Single-Mode Optical Fibers. *Journal of Lightwave Technology, Vol. 31, Issue 12, pp. 2008-2017*, 31(12):2008–2017, jun 2013.

[24] M. Oppelt, M. Baumann, R. Bergmann, E. Beyreuther, K. Brüchner, J. Hartmann, L. Karsch, M. Krause, L. Laschinsky, E. Leßmann, M. Nicolai, M. Reuter, C. Richter, A. Sävert, M. Schnell, M. Schürer, J. Woithe, M. Kaluza, and J. Pawelke. Comparison study of in vivo dose response to laser-driven versus conventional electron beam. *Radiation and Environmental Biophysics*, 54(2):155–166, may 2015.

[25] E. E. Ozkan. Plasma and tissue insulin-like growth factor-I receptor (IGF-IR) as a prognostic marker for prostate cancer and anti-IGF-IR agents as novel therapeutic strategy for refractory cases: A review, sep 2011.

[26] H. Rezazadeh, A. Neirameh, M. Eslami, A. Bekir, and A. Korkmaz. A sub-equation method for solving the cubic-quartic NLSE with the Kerr law nonlinearity. *Modern Physics Letters B*, 33(18), jun 2019.

[27] T. Sakimoto, M. I. Rosenblatt, and D. T. Azar. Laser eye surgery for refractive errors, apr 2006.

[28] R. Samad, L. Courrol, S. Baldochi, and N. Vieir. Ultrashort Laser Pulses Applications. In *Coherence and Ultrashort Pulse Laser Emission*. InTech, nov 2010.

[29] P. Singh, J. M. Alex, and F. Bast. Insulin receptor (IR) and insulin-like growth factor receptor 1 (IGF-1R) signaling systems: Novel treatment strategies for cancer. *Medical Oncology*, 31(1), 2014.

[30] R. A. Snavely, M. H. Key, S. P. Hatchett, I. E. Cowan, M. Roth, T. W. Phillips, M. A. Stoyer, E. A. Henry, T. C. Sangster, M. S. Singh, S. C. Wilks, A. MacKinnon, A. Offenberger, D. M. Pennington, K. Yasuike, A. B. Langdon, B. F. Lasinski, J. Johnson, M. D. Perry, and E. M. Campbell. Intense high-energy proton beams from petawatt-laser irradiation of solids. *Physical Review Letters*, 85(14):2945–2948, oct 2000.

[31] P. Sprangle, E. Esarey, and B. Hafizi. Intense laser pulse propagation and stability in partially stripped plasmas. *Physical Review Letters*, 79(6):1046–1049, jan 1997.

[32] P. Sprangle, E. Esarey, and A. Ting. Nonlinear interaction of intense laser pulses in plasmas. *Physical Review A*, 41(8):4463–4469, apr 1990.

[33] P. Sprangle and B. Hafizi. Guiding and stability of short laser pulses in partially stripped ionizing plasmas. In *Physics of Plasmas*, volume 6, pages 1683–1689. American Institute of PhysicsAIP, may 1999.

[34] P. Sprangle, B. Hafizi, and J. R. Peñano. Laser pulse modulation instabilities in plasma channels. *Physical Review E - Statistical Physics, Plasmas, Fluids, and Related Interdisciplinary Topics*, 61(4):4381–4393, apr 2000.

[35] P. Sprangle, J. R. Peñano, and B. Hafizi. Propagation of intense short laser pulses in the atmosphere. *Physical Review E - Statistical Physics, Plasmas, Fluids, and Related Interdisciplinary Topics*, 66(4):21, 2002.

[36] P. Sprangle, A. Ting, and C. M. Tang. Analysis of radiation focusing and steering in the free-electron laser by use of a source-dependent expansion technique. *Physical Review A*, 36(6):2773–2781, sep 1987.

[37] W. M. Steen and J. Mazumder. *Laser material processing: Fourth edition*. Springer London, 2010.

[38] R. Toth, J. C. Kieffer, S. Fourmaux, T. Ozaki, and A. Krol. In-line phase-contrast imaging with a laser-based hard x-ray source. *Review of Scientific Instruments*, 76(8):1–6, aug 2005.

[39] M. H. Weik and M. H. Weik. Gaussian pulse. In *Computer Science and Communications Dictionary*, pages 676–676. Springer US, 2000.

[40] J. Wenz, S. Schleede, K. Khrennikov, M. Bech, P. Thibault, M. Heigoldt, F. Pfeiffer, and S. Karsch. Quantitative X-ray phase-contrast microtomography from a compact laser-driven betatron source. *Nature Communications*, 6(1):1–6, jul 2015.

[41] B. Yedierler. Remote ionization by a short pulse laser beam propagating in the atmosphere. *Physics of Plasmas*, 15(7):073107, jul 2008.

[42] B. Yedierler. Nonlinear longitudinal compression of short laser pulses in the atmosphere. *Physics of Plasmas*, 16(5):053104, may 2009.

[43] B. Yedierler. Curvature aided long range propagation of short laser pulses in the atmosphere. *Physics of Plasmas*, 20(3), 2013.

[44] A. Yogo, T. Maeda, T. Hori, H. Sakaki, K. Ogura, M. Nishiuchi, A. Sagisaka, H. Kiriyama, H. Okada, S. Kanazawa, T. Shimomura, Y. Nakai, M. Tanoue, F. Sasao, P. R. Bolton, M. Murakami, T. Nomura, S. Kawanishi, and K. Kondo. Measurement of relative biological effectiveness of protons in human cancer cells using a laser-driven quasimonoenergetic proton beamline. *Applied Physics Letters*, 98(5):053701, jan 2011.

[45] A. Yogo, K. Sato, M. Nishikino, M. Mori, T. Teshima, H. Numasaki, M. Murakami, Y. Demizu, S. Akagi, S. Nagayama, K. Ogura, A. Sagisaka, S. Orimo, M. Nishiuchi, A. S. Pirozhkov, M. Ikegami, M. Tampo, H. Sakaki, M. Suzuki,

I. Daito, Y. Oishi, H. Sugiyama, H. Kiriyama, H. Okada, S. Kanazawa, S. Kondo, T. Shimomura, Y. Nakai, M. Tanoue, H. Sasao, D. Wakai, P. R. Bolton, and H. Daido. Application of laser-accelerated protons to the demonstration of DNA double-strand breaks in human cancer cells. *Applied Physics Letters*, 94(18):181502, may 2009.

[46] W. Yu, M. Y. Yu, J. Zhang, L. J. Qian, X. Yuan, P. X. Lu, R. X. Li, Z. M. Sheng, J. R. Liu, and Z. Z. Xu. Long-distance propagation of intense short laser pulse in air. *Physics of Plasmas*, 11(11):5360–5363, nov 2004.

[47] Y. Yu, S. Bai, S. Wang, and A. Hu. Ultra-Short Pulsed Laser Manufacturing and Surface Processing of Microdevices, dec 2018.